CHAPTER 5 RESULTS AND DISCUSSIONS

5.1 INTRODUCTION

This chapter presents the overall findings of the experimental modal analysis and finite element (FE) study with the different boundary conditions, damage identification and model validation. The boundary condition is a major factor which influences the modal parameters. The natural frequencies, mode shapes and model damping obtained from the experiment are studied in order to determine the effect of boundary conditions, namely free-free (FF), spring support (SS) and fixed roller (FR). The modal parameters obtained are correlated to the state of damage in the beam induced by a saw cut at its soffit. The depth of the cut was increased so as to obtain the different levels of severity of the damage. Changes in natural frequencies, curvature mode shapes, modal assurance criterion (MAC) and coordinate modal assurance criterion (COMAC) are used as damage indicators to evaluate and detect the crack location. A new algorithm is also proposed to evaluate and detect the crack location for the single and dual crack cases. Finally, the model validation between experimental model and analytical model was performed by updating the FE model.

5.2 VALIDATION CHECK

In the process of modal testing, the measured frequency response functions (FRFs) were acquired using a dynamic analyzer. The modal data such as natural frequencies, mode shapes and modal damping were obtained by performing curve fitting on a number of measured FRFs. The frequency domain parameter identification technique in ICATS was utilised to estimate the modal parameters. The extracted natural frequencies and mode shapes were used to evaluate the state of the structure and

to predict the damage location in this study. Before using these modal data, a check was done in order to ensure the quality and validity of the modal data.

In this investigation, reciprocal modal vector [23] in ICATS was utilised to verify the modal data by comparing the measured FRFs (raw data) with the synthesized FRFs obtained via modal summation. The orthogonality of the modal data with respect to the corresponding measured FRFs was assessed using Equation 5.1

$$\left[\{\alpha(\omega_1)\}_p, \{\alpha(\omega_2)\}_p, \ldots\ldots \{\alpha(\omega_s)\}_p\right]^T \{\chi\}_r = \phi_{pr} \begin{Bmatrix} \frac{1}{\omega_r^2 - \omega_1^2} \\ \frac{1}{\omega_r^2 - \omega_2^2} \\ \ldots\ldots \\ \frac{1}{\omega_r^2 - \omega_s^2} \end{Bmatrix} \qquad \text{Equation 5.1}$$

where

$\alpha(\omega_s)$ is the receptance FRF at s excitation frequencies.

ϕ_{pr} is the mass normalized mode shape at mode r in the p-th column.

$\{\chi\}$ is the reciprocal vector matrix.

ω is the natural frequency.

The output of the reciprocal modal vector matrix should be close to unity indicating good quality modal data.

Figure 5.1 shows the reciprocal modal vector matrices of the undamaged beam for free-free, spring and roller support conditions. It was observed that the boundary condition did affect the quality of modal data especially for the lower modes. The diagonal values of the matrix drop from 1.0 to 0.5 for modes 2 and 4 as the support conditions became stiffer. The reduction indicated the poor quality of modal data obtained for the particular mode. Although some modes fell within the poor quality range, the overall results, especially the higher modes were still exhibiting reasonable quality and acceptable modal data for further investigation.

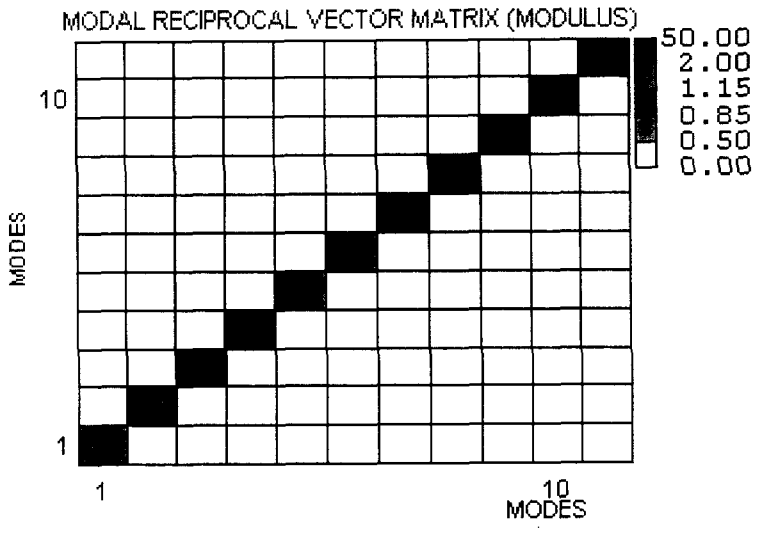
MODAL RECIPROCAL VECTOR MATRIX (MODULUS)
50.00
2.00
1.15
0.85
0.50
0.00
10
1
MODES
1
10
MODES

(a) FF

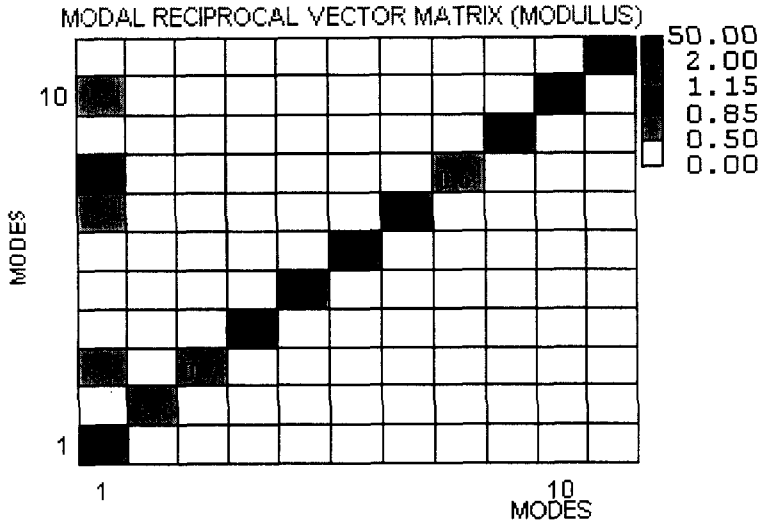
MODAL RECIPROCAL VECTOR MATRIX (MODULUS)
50.00
2.00
1.15
0.85
0.50
0.00
10
1
MODES
1
10
MODES

(b) SS

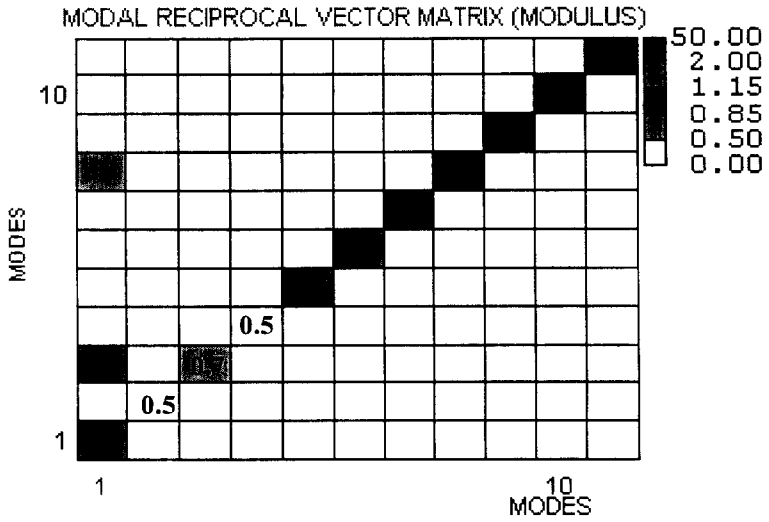

(c) FR

Figure 5.1 Reciprocal modal vector matrix for different boundary condition

5.3 BOUNDARY CONDITIONS EFFECT

According to Timoshenko [1], a typical normal function for transverse free vibration of a simple beam can be written as

$$X = C_1 \sin \lambda x + C_2 \cos \lambda x + C_3 \sinh \lambda x + C_4 \cosh \lambda x \qquad \text{Equation 5.2}$$

where the four amplitude constants C_1, C_2, C_3 and C_4, and the eigenvalue λ are determined in each particular case from the boundary conditions at the ends of the beam. Based on the above typical function, the modal properties i.e natural frequencies, mode shapes and damping, will change when there is change in boundary conditions.

5.3.1 NATURAL FREQUENCY

In general, the stiffer the support condition, the higher will be the natural frequency, when all other physical properties remained unchanged. However, Chowdhury [6] found that the stiffer the support condition, the lower will be the natural frequency, especially for the lower modes. Similarly, the results of this investigation confirmed this trend. Furthermore, it was proven by Timoshenko [1] that the frequency of flexural mode for free-free beam is higher than simply supported beam as given in

Equation 2.15 and 2.8 respectively. Tables 5.1a and 5.1b present the changes in natural frequencies for the first six flexural modes and the first five torsional modes. It was apparent that the changes in natural frequencies for the first two flexural modes were significant as the boundary conditions became stiffer. The natural frequencies of the flexural modes 1 and 2 for the free-free end conditions were 83.66Hz and 230.13Hz respectively. It subsequently reduced to 64.39Hz and 187.38Hz for the spring supports and 31.02Hz and 133.12Hz for the fixed roller supports, respectively. However, the change in boundary condition had an insignificant effect on the natural frequencies for the higher modes which exhibited a slight increase in the values.

Boundary conditions	FF	SS		FR	
	Degree of support stiffness → (Increase)				
Natural frequencies of undamaged beams	Frequency	Frequency	Change in freq. (%)	Frequency	Change in freq. (%)
	83.66	64.39	-23.03	31.02	-62.92
	230.13	187.38	-18.57	133.12	-42.15
	451.38	488.90	8.31	489.74	8.50
	746.25	760.98	1.97	763.13	2.26
	1113.29	1125.83	1.13	1122.99	0.87
	1549.05	1555.24	0.40	1555.99	0.45

Table 5.1a Natural frequencies for flexural modes

Boundary conditions	FF	SS		FR	
	Degree of support stiffness → (Increase)				
Natural frequencies of undamaged beams	Frequency	Frequency	Change in freq. (%)	Frequency	Change in freq. (%)
	350.61	383.36	9.34	379.65	8.28
	708.76	726.91	2.56	726.61	2.52
	1085.66	1099.07	1.24	1098.96	1.23
	1485.70	1497.36	0.78	1497.59	0.80
	1917.44	1925.16	0.40	1925.40	0.41

(+ve is increasing and –ve is reduction)

Table 5.1b Natural frequencies for torsional modes

5.3.2 MODE SHAPE

Mode shapes are associated with structural resonance. They change with the physical properties or boundary conditions of the structure [11]. Figures 5.2 and 5.3 show the variation of the mode shapes amplitude for the flexural modes and torsional modes for different support conditions. In these figures the imaginary parts of the FRF (residues) obtained from the curve fitting were plotted to obtain deflected shape of the beam. These imaginary parts are proportional to the deflection of the test object and can be used to detect the variation in the amplitude due to different support conditions.

The amplitude of flexural and torsional modes in the free-free, spring and fixed roller support obtained from model testing are summarized in Figure 5.2 and Figure 5.3. Theoretically, the amplitudes at the edges for the roller support should be zero. However, the amplitude of fixed roller beam is not equal to zero. This is due to the fixed roller support, as shown in Figure 4.1, is not fully constraint in vertical direction and it consists space for the upward movement.

Referring to Figure 5.2, it was apparent that the stiffer the support, the smaller the amplitude of vibration, especially for the lower modes. This phenomenon can be explained by the freedom of movement of the beam under different support media. In the case of free-free condition, the beam has more space to move while in the case of stiffer support, like a steel roller, the movement of the beam is restricted by the end of the support. As a result, higher amplitudes of vibration were observed in the free-free beam. Subsequently the amplitude reduced from the free-free condition to spring support and was even less in the fixed roller support. This indicated that the degree of freedom of the beam is inversely proportional to the support stiffness.

A similar result was also reported by Chowdhury [6]. The author had carried out modal testing on an aluminum plate with different boundary conditions. The aluminum

PERPUSTAKAAN UNIVERSITI MALAYA

plate was laid over four independent supports: free-free, sand, concrete and steel. It was observed that the less stiffer the support material the higher the mode shape amplitude.

For flexural modes higher than the third, the change in boundary condition did not significantly affect the amplitude which exhibited a slight reduction or remained unchanged. Similar results were also obtained for the torsional modes where the amplitude of other two support conditions were as close as that of the free-free condition.

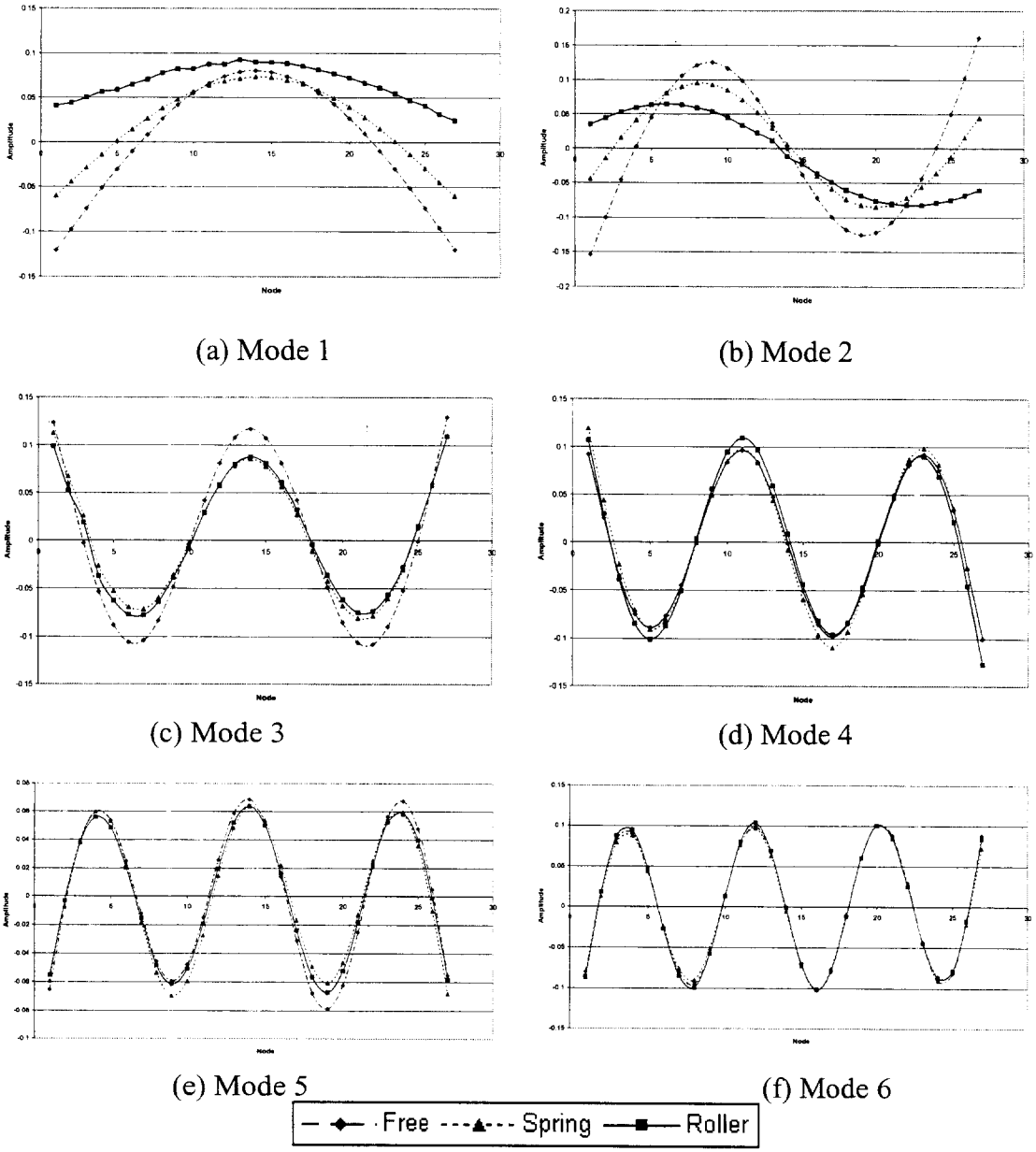

Figure 5.2 Amplitude of mode shapes for flexural modes

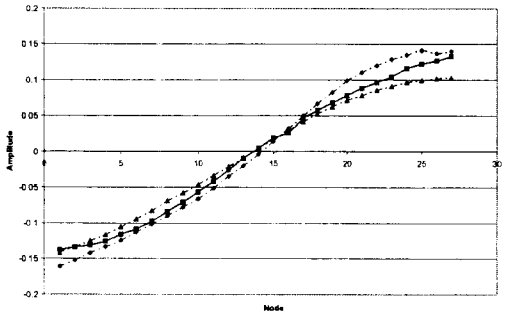

(a) Mode 1

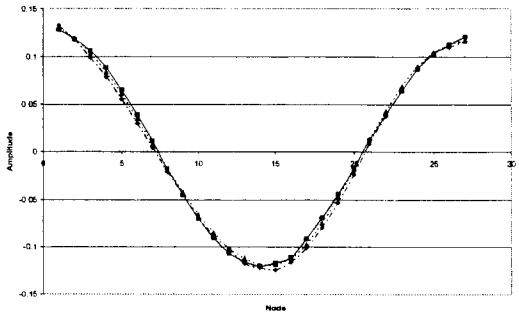

(b) Mode 2

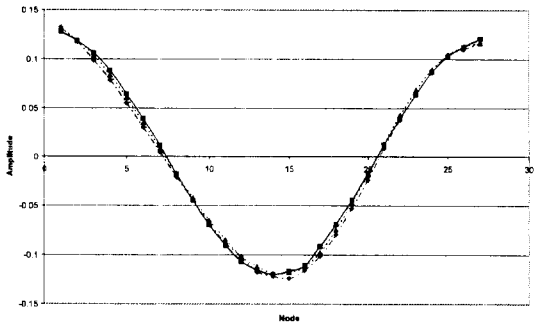

(c) Mode 3

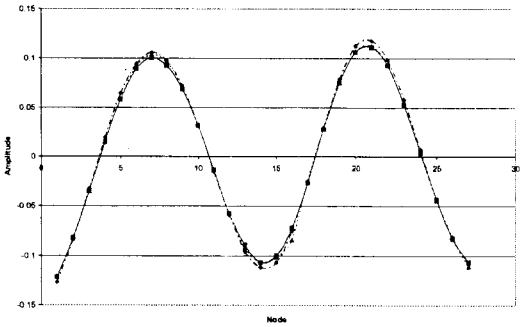

(d) Mode 4

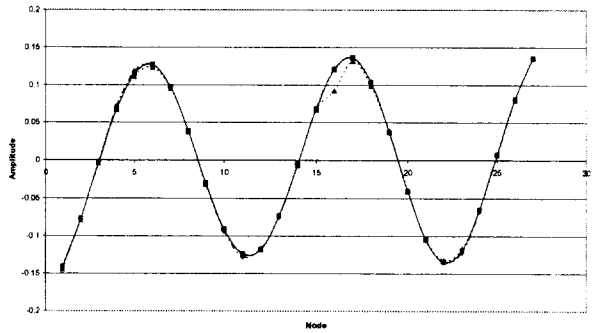

(e) Mode 5

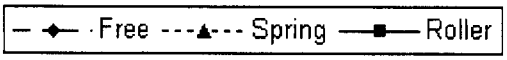

Figure 5.3 Amplitude of mode shapes for torsional modes

5.3.3 DAMPING RATIO

Damping exists in all vibratory systems whenever there is energy dissipation. This is true for mechanical structures even though inherently most are lightly damped. In case of free vibration, the loss of energy from damping in the system results in the decay of the amplitude of motion. As for cases of forced vibration, loss of energy is balanced by the energy supplied by excitation. In either situation, the effect of damping is to remove energy from the system. The variations of the damping ratio of flexural modes and torsional modes due to changes in boundary conditions are illustrated in Figure 5.4.

Basically, the ratios shown in Figure 5.4 represent the damping characteristic of the test beams which are associated with energy dissipation or energy loss within the system. Theoretically without other changes except the boundary condition, if the beam has a low stiffness support condition, the tendency is for lower energy to be imparted by the excitation force. This would be sufficient to balance the energy dissipation of the low stiffness of the support. Correspondingly, a higher energy is needed for high support stiffness to balance the higher energy dissipation within the system. Consequently, it is expected that the trend for the damping ratio obtained should increase as the boundary condition gets stiffer.

Referring to Figure 5.4a, a consistent trend in the damping ratios was observed for the flexural modes due to changes in boundary condition. It was apparent that the damping ratios increased when the boundary condition changed from free-free to spring to fixed roller support, with the exception of modes 1 and 5. The damping ratios of modes 1 and 5 were 1.1%, 0.8% and 6.79% and 0.11%, 0.55% and 0.38% respectively for the free-free, spring and fixed roller support conditions. However for torsional modes, differences in the damping ratios were only significant in mode 1 while other modes exhibited only a slight change in value. This can be probably due to the fact that

the torsional mode is less sensitive compared to the flexural mode when there are changes in boundary conditions. Moreover, for higher modes, damping ratios were less affected by the stiffness of the boundary conditions.

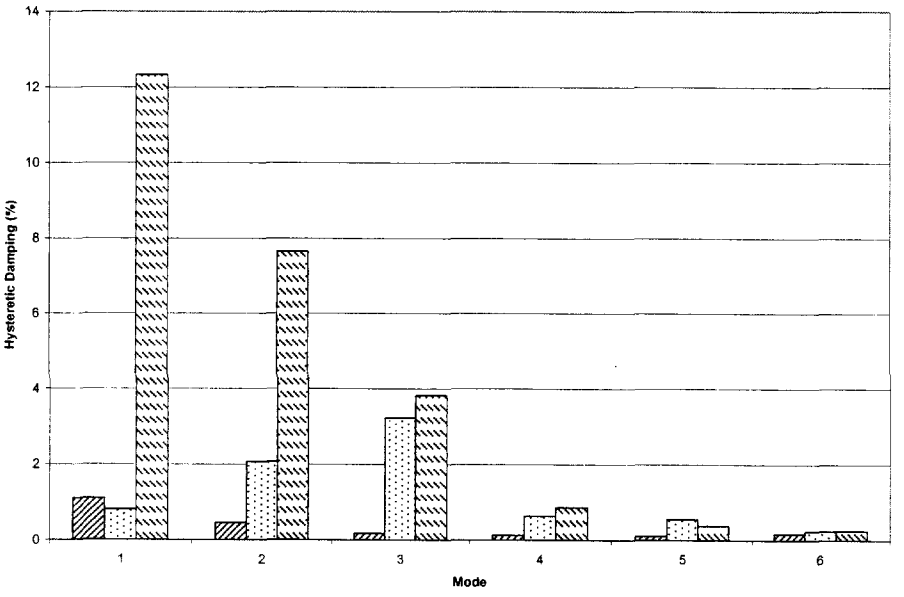

(a) Flexural modes

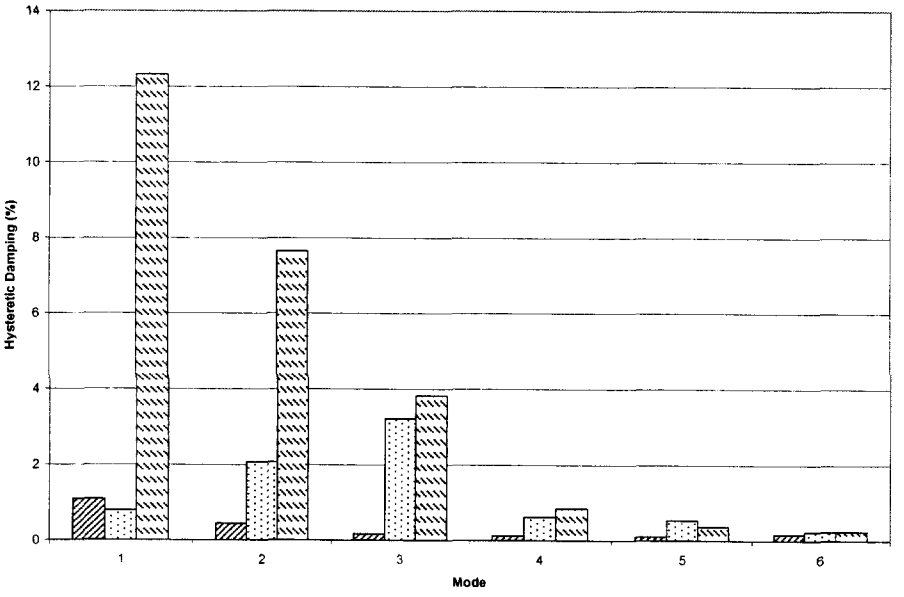

(b) Torsional modes

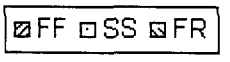

Figure 5.4 Damping ratio for different boundary conditions

5.4 DAMAGE IDENTIFICATION

When a system is subjected to a certain degree of damage or deterioration, it experiences a change on the physical properties namely the mass, damping and in particular the stiffness of the structure. The basic idea underlying damage identification using modal parameters such as natural frequencies, mode shapes and modal damping are that they are functions of the physical properties of the structure. Consequently, the changes in physical properties will cause changes in modal properties. Thus, the investigation on modal analysis was carried out to observe the change which was related to the damage induced by a saw cut to simulate an open crack at the soffit of the steel beam as shown in Figure 5.5.

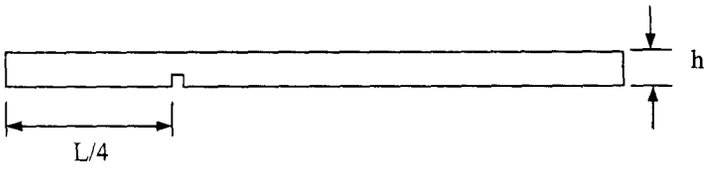

Figure 5.5 Crack location on the steel beam

The modal damping based damage identification technique is not discussed due to the inconsistencies in the results and inaccuracy in its measurement. According to Salawu [16] and Kato [32], the inconsistency of changes in damping ratios was obtained due to measurement error introduced by background noise as well as by the interference of the measuring equipment. In addition, the damping ratio is estimated from the half-power bandwidth of the frequency spectra after undergoing the curve fitting process. Thus, the original signal is modified and coupled with the curve fitting process, a less accurate estimation of the damping ratio is acquired.

5.4.1 FREQUENCY CHANGES

The natural frequency of a structure bears a direct relationship with the structural stiffness. For an undamped vibrating system with mass m, the relationship can be written as

$$\omega_i \propto \sqrt{\frac{EI}{m}} \qquad \text{Equation 5.2}$$

where EI is the stiffness in the structure and ω_i is the angular frequency for mode i. Based on Equation 5.2, reduction in stiffness (EI) of a structure leads to reduction in natural frequencies for the corresponding modes. Thus the natural frequency of a vibrating system is a useful global parameter to indicate the occurrence of damage and to evaluate the severity or state of damage in the structure.

The changes in natural frequencies are also dependant on the nature and severity of the damage; in particular it's location. As stated in the literature review of Salawu [4], the degree of reduction in natural frequency is dependent on the position of the defect relative to the mode shape for a particular mode of vibration. The reduction becomes more important when the crack is located at the high curvature region for the modes under consideration. The reduction of any modes is also proportional to the square of the modal strain value [5]. In other words, the reduction in frequency is maximum if the crack is located at the peak or trough of the strain mode and minimum if the crack is located at the node of the strain mode. Therefore, natural frequency changes are not only to monitor structural conditions but also useful to identify the damage location.

5.4.1.1 SEVERITY CHECK

The natural frequencies of flexural and torsional modes in the free-free, spring and simply support conditions obtained from modal testing are summarized in Tables 5.2 and 5.3. The frequencies of flexural mode 6 B6 and torsional mode 4 T4 at 0.5h cut damage level were omitted due to identification problems for the closely spaced between the two modes. This is due to the smaller impact of the damage on the T4 than that on the B6, which causes the changes in sequence between T4 and B6 during the

damaging process. The flexural mode 2 for case 0.61h cut in the fixed roller support condition was not obtainable, probably due to the distortion caused by a rigid body mode and noise.

The relative drop of natural frequencies with respect to the control state or undamaged state is illustrated in Tables 5.2 and 5.3. It was observed that the natural frequencies of the beam experienced reductions for all the boundary conditions when cracking was induced. It was also apparent that the higher the degree of the damage, the higher the drop in natural frequency. However, for lower modes of the spring and fixed roller support conditions the trend of change in natural frequencies was inconsistent when the damage induced was small. The inconsistent trend can be explained since the change in natural frequencies was more affected by support stiffer rather the damage induced.

By comparing the percentage drop in natural frequencies, the flexural modes were higher than the torsional modes. In the case of the 0.67h cut, the average percentage drop in natural frequencies for the flexural modes in free-free, spring and fixed roller support conditions were 6.81%, 5.92% and 4.89% respectively, but for the torsional modes the corresponding averages were only 1.2%, 1.25% and 1.35%. This indicated that flexural modes were more sensitive compared to the torsional modes in detecting crack damage in the beam.

From the case of 0.17h cut to 0.5h cut, the percentage drop in flexural frequencies was rather small for all the boundary conditions. However, at 0.61h cut the second and third flexural frequencies decreased much more dramatically. This may be explained by the formation of a plastic hinge at the crack location, which causes a higher drop in flexural frequencies. A similar trend was also reported in a study by Wen [27]. The author carried out vibration measurements on a reinforced concrete beam where the cracking was induced by a series of step load tests. The drop in flexural

frequencies was small from the second load step to the fifth. At the ultimate damage state (the sixth or last load step), the drop in first flexural frequencies was dramatically much more than the previous state because of the formation of a plastic hinge.

In addition, the stiffness of the boundary condition also affects the drop in natural frequencies due to the damage in the structure. For the same level of damage that is the 0.67h cut, the percentage drop in natural frequencies of flexural mode 1 for the free-free, spring and fixed roller support conditions were 6.88%, 4.95% and 3.56% respectively, while for the flexural mode 2 they were 13.56%, 11.76% and 3.62% respectively. The percentage drop in natural frequencies reduced as the support stiffness increased which implied a decrease in sensitivity for damage detection. A similar trend was also observed for the less severe damage cases of the 0.39h mm cut, 0.5h cut and 0.61h cut.

5.4.1.2 DAMAGE LOCATION

As mentioned earlier in section 5.4.1.1, the percentage drop in natural frequencies of the torsional modes was not as sensitive as the flexural modes. Hence, only the flexural modes were chosen as an indicator to identify the damage location in the beam using the changes in natural frequencies. Figure 5.6 shows the percentage drop in natural frequencies of the different damage levels for the free-free, spring and fixed roller support conditions. The negative values presented in the graphs were ignored since the natural frequency is inversely proportional to stiffness of the structure, as shown in Equation 5.2. It was noticed that the changes in natural frequencies was different for every mode for all the boundary conditions at every damage level. It was therefore inferred that the percentage drop in natural frequencies was also a function of the crack location.

Boundary condition	Modes / Depth of cut	1		2		3		4		5		6	
		Freq.	Drop (%)	Freq.	Drop (%)	Freq.	Drop (%)	Freq.	Drop (%)	Freq.	Drop (%)	Freq.	Drop (%)
FF	0	83.7		230.1		451.4		746.3		1113.3		1549.1	
	0.17h	83.4	0.33	228.9	0.52	449.4	0.43	745.8	0.06	1111.7	0.14	1541.4	0.49
	0.28h	83.1	0.67	227.0	1.37	446.5	1.08	745.2	0.14	1109.4	0.35	1529.7	1.25
	0.39h	82.8	1.08	223.0	3.10	440.8	2.33	744.4	0.25	1105.6	0.69	1510.1	2.52
	0.50h	81.8	2.28	216.6	5.87	433.1	4.06	742.8	0.47	1099.1	1.27	-	-
	0.61h	79.9	4.46	205.8	10.57	420.9	6.75	740.6	0.76	1088.4	2.24	1432.9	7.50
	0.67h	77.9	6.88	198.9	13.56	414.5	8.17	739.5	0.90	1082.3	2.78	1412.0	8.85
SS	0	64.4		187.4		488.9		761.0		1125.8		1555.2	
	0.17h	64.1	0.52	187.7	-0.15	489.4	-0.10	761.9	-0.12	1125.4	0.04	1548.5	0.43
	0.28h	64.2	0.33	184.7	1.43	486.3	0.53	761.0	-0.01	1143.0	-1.52	1537.1	1.16
	0.39h	63.7	1.01	181.3	3.23	474.7	2.91	758.3	0.35	1117.9	0.70	1516.1	2.52
	0.50h	63.3	1.71	179.8	4.03	470.7	3.72	757.3	0.48	1114.0	1.05	-	-
	0.61h	62.1	3.58	171.8	8.32	457.4	6.43	754.4	0.86	1098.3	2.44	1439.7	7.43
	0.67h	61.2	4.95	165.3	11.76	456.1	6.70	754.1	0.90	1097.8	2.49	1419.3	8.74
FR	0	31.0		133.1		489.7		763.1		1123.0		1556.0	
	0.17h	31.7	-2.12	132.2	0.70	485.4	0.89	762.8	0.04	1121.7	0.11	1548.6	0.48
	0.28h	31.2	-0.52	129.8	2.48	480.0	1.99	760.8	0.31	1119.0	0.36	1536.9	1.23
	0.39h	31.4	-1.24	133.1	0.04	479.3	2.14	760.9	0.29	1115.8	0.64	1517.2	2.50
	0.50h	31.0	-0.06	129.6	2.67	472.5	3.52	758.5	0.60	1109.6	1.19	-	-
	0.61h	30.3	2.33	-	-	444.3	9.29	755.7	0.97	1099.2	2.12	1440.3	7.43
	0.67h	29.9	3.56	128.3	3.62	441.4	9.87	755.5	0.99	1094.8	2.51	1419.6	8.77

Degree of support stiffness (increase) →

Table 5.2 Natural frequencies for flexural modes

Boundary condition	Modes / Depth of cut	1		2		3		4		5	
		Freq.	Drop (%)	Freq.	Drop (%)	Freq.	Drop (%)	Freq.	Drop (%)	Freq.	Drop (%)
FF	0	350.6		708.8		1085.7		1485.7		1917.4	
	0.17h	350.1	0.15	707.1	0.23	1084.4	0.12	1484.4	0.09	1914.4	0.16
	0.28h	349.6	0.28	705.6	0.44	1083.3	0.22	1483.3	0.16	1912.0	0.29
	0.39h	349.2	0.40	703.7	0.72	1081.6	0.38	1479.2	0.44	1908.0	0.49
	0.50h	348.6	0.58	701.8	0.98	1079.6	0.56	-	-	1904.5	0.68
	0.61h	348.3	0.65	700.1	1.22	1077.5	0.75	1466.0	1.33	1901.2	0.85
	0.67h	347.8	0.81	699.7	1.28	1076.0	0.89	1454.2	2.12	1900.2	0.90
SS	0	383.4		726.9		1099.1		1497.4		1925.2	
	0.17h	384.8	-0.38	725.9	0.14	1098.0	0.09	1496.8	0.04	1922.9	0.12
	0.28h	382.6	0.20	723.7	0.44	1096.6	0.22	1495.0	0.16	1919.8	0.28
	0.39h	380.7	0.69	720.6	0.87	1093.8	0.48	1489.8	0.51	1915.2	0.52
	0.50h	379.7	0.96	718.9	1.10	1092.4	0.61	-	-	1911.8	0.69
	0.61h	379.4	1.04	717.3	1.32	1090.2	0.81	1475.9	1.43	1908.6	0.86
	0.67h	379.5	1.02	717.1	1.35	1090.3	0.80	1464.4	2.20	1908.0	0.89
FR	0	379.7		726.6		1099.0		1497.6		1925.4	
	0.17h	378.3	0.35	724.2	0.34	1097.2	0.16	1496.1	0.10	1922.7	0.14
	0.28h	375.9	0.98	721.7	0.68	1094.9	0.37	1493.8	0.25	1919.2	0.32
	0.39h	377.4	0.59	721.1	0.76	1094.3	0.43	1490.5	0.47	1916.1	0.48
	0.50h	376.1	0.93	718.5	1.11	1092.3	0.61	-	-	1912.0	0.69
	0.61h	374.3	1.40	716.0	1.46	1089.6	0.85	1475.4	1.48	1908.3	0.89
	0.67h	375.2	1.18	715.9	1.48	1088.4	0.96	1464.1	2.23	1907.8	0.91

Degree of support stiffness (increase) →

Table 5.3 Natural frequencies for torsional modes

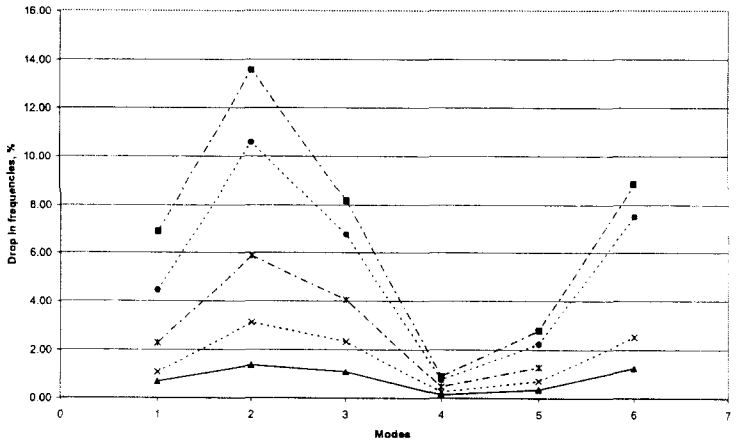

(a) Free -Free

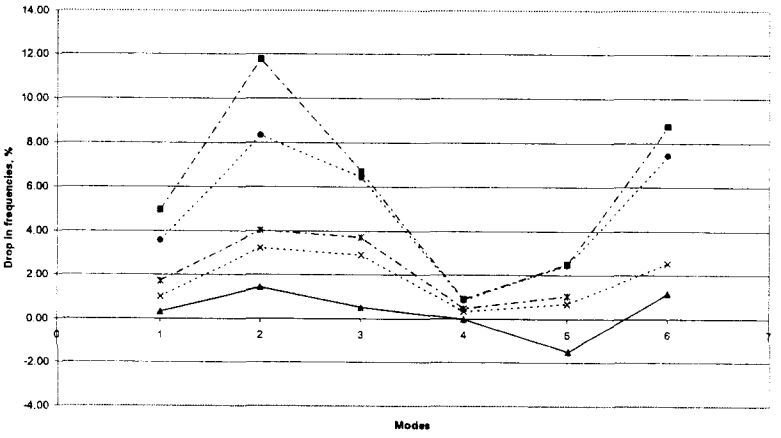

(b) Spring Support

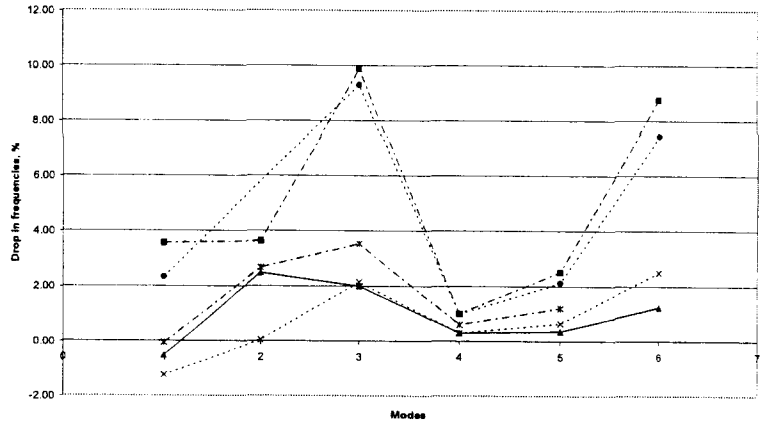

(c) Fixed Roller

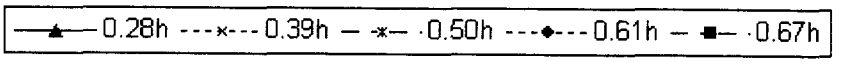

Figure 5.6 Comparison of percentage drop in flexural frequencies for (a) free-free, (b) spring support and (c) fixed roller

Referring to Figure 5.6, particular modes always returned the minimum and maximum percentage drop in natural frequencies, as the damage level increased. This consistent trend was noticeable when the cut damage was 0.17h for free-free. For spring and fixed roller support conditions, the trend was also noticeable when the cut damage was 0.28h. For all the boundary conditions, mode 4 returned the minimum percentage drop while different modes returned the maximum percentage drop. For free-free and spring support conditions mode 2 returned the maximum percentage drop while for the fixed roller support it was mode 3. This shift was influenced by the support stiffness. The stiffer support of the fixed roller support condition reduced the sensitivity of percentage drop in natural frequency for the first two modes due to the damage, as mentioned earlier in Section 5.4.1.1.

According to Narayana [5], the frequency change is proportional to the square of the modal strain. The modal strain or bending strain is also directly related to the curvature as given by

$$\varepsilon = y\nu'' \qquad \text{Equation 5.3}$$

where ε is strain, ν'' is curvature mode shape and y is distance from the neutral axis. This suggests that the possible crack location of free-free and spring supports was located at the high curvature zone of mode 2 and the low curvature zone of mode 4. In other words, the crack location can be estimated at location near to the 0.28L, as shown in Figures 5.7a and 5.7b. For fixed roller support condition, the possible crack location was located either close to 0.28L or 0.5L which was the location of high curvature for mode 3 and the low curvature for mode 4, as shown in Figures 5.7c. The 0.5L was not possible crack location because the percentage drop for the sixth flexural frequency was high although the curvature was low. Thus the damaged detection based on the percentage drop related to the curvature gave close approximation of the crack location which was located at 0.25L.

The high sensitivity of changes in natural frequencies due to the damage made it suitable to be used as a damage indicator. Moreover, changes in natural frequencies are also applicable for the less severe case where it can detect the damage location up to 0.17h cut for the free-free condition and 0.28h cut for the spring and fixed roller support conditions. However, the symmetry of the beam provided symmetrical mode shapes with two possible damage locations can be obtained either at 0.28L or 0.72L.

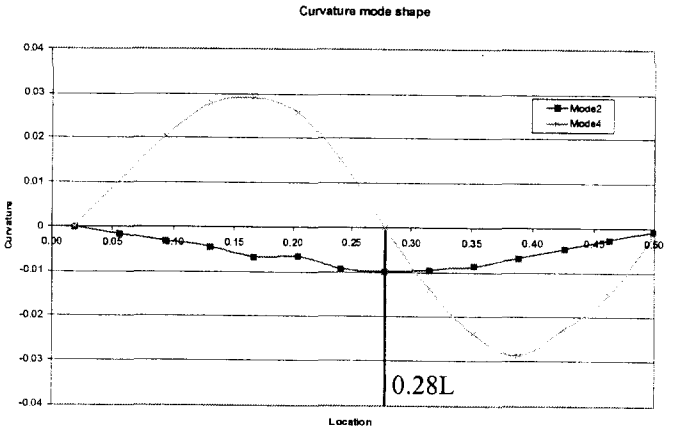

(a) Free-Free

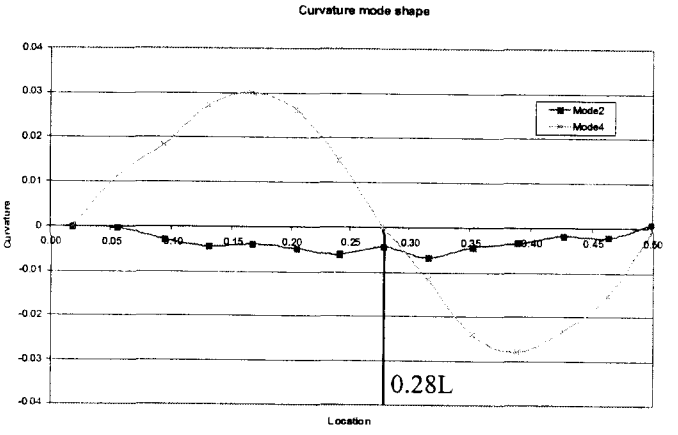

(b) Spring Support

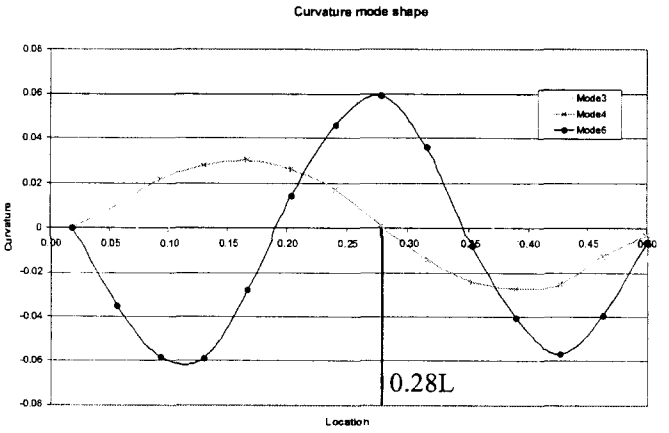

(c) Fixed Roller

Figure 5.7 Curvature mode Shapes for (a) free-free, (b) spring support and (c) fixed roller

5.4.2 MODE SHAPE CHANGES

Mode shapes express the oscillation of an undamped single degree of freedom (SDOF) system when it is subjected to an initial perturbation. Subsequently when it is left to move freely, the system will oscillate about the static equilibrium position. This is referred to as its natural modes of vibration. Mathematically speaking, the mode shape of a dynamic system is characterized through a unique property described by its free vibration natural frequency.

For this investigation, the first six flexural mode shapes of the free-free beam at different levels of damage are shown in Figure 5.8. It was apparent that the crack at the quarter span did influence the mode shape behavior. A clear trend can still be seen due to the damage level in Figure 5.8. The nodes were shifted slightly towards the damage zone and the relative mode amplitudes were changed at the damage location. When the cut was greater than 0.61h, the changes in mode shapes were clearly noticeable in modes 5 and 6 as compared with the control. The nodes shifted significantly towards the damage zone. However, not only at the damage location, displacements in mode shapes and changes in relative amplitude were noticeable not only at the damage location but

also along the length of the beam. This indicated that the formation of a plastic hinge significantly affected the mode shape, especially for the higher modes.

As the support stiffness of the beam increased, the mode shape was affected not only by the damage induced but also by the stiffness of the supports. Figure 5.9 shows the plot of the first two flexural modes at different levels of damage for free-free, spring and fixed roller support for purpose of comparison. Other modes were omitted since the support conditions had less significant effect on the higher modes, as mentioned in section 5.3.2 and their results were similar to the free-free condition.

Referring to Figure 5.9, the mode shapes of the spring and fixed roller support did not present a clear trend as compared with the free-free. For spring and fixed roller support, the displacement in mode shape and changes in relative amplitude were inconsistent due to the damage level. It was also observed that the changes occurred along the length of the beam although it was not the effect of formation of a plastic hinge. Therefore, it was inferred that the support condition did influence the mode shape and its effect was more dominant than the damage induced when stiffer support condition was encountered.

Based on above results, the changes in mode shape indicated the occurrence of damage but it did not give any clear indication of the damage location. In a study by Narayana [5], the analytical results presented insignificant amplitude increases at the crack location due to damage of up to 50% reduction in beam depth. As a result, the above trend and amplitude changes at the crack location were not applicable to detect and locate the damage in the structure. Moreover the stiffer the support condition in the structure, the less smooth the mode shape obtained.

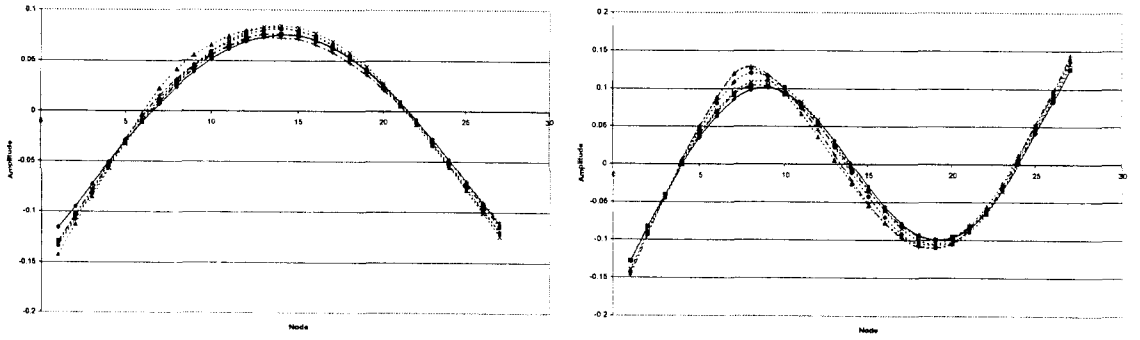

(a) Mode 1 (b) Mode 2

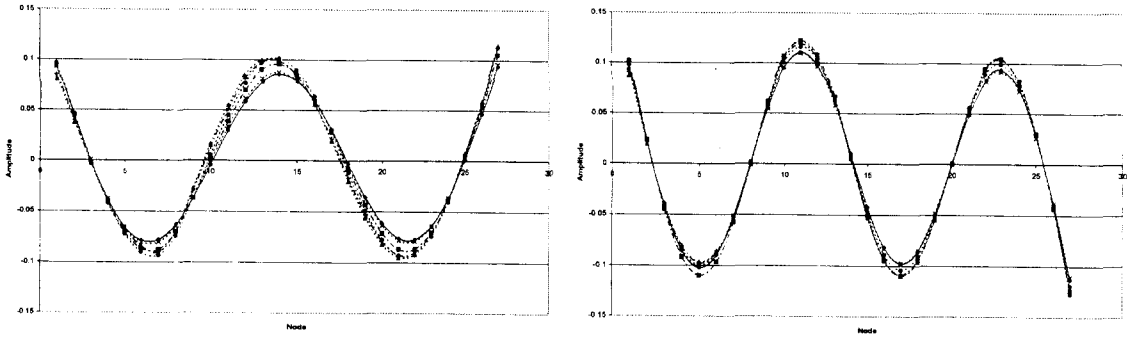

(c) Mode 3 (d) Mode 4

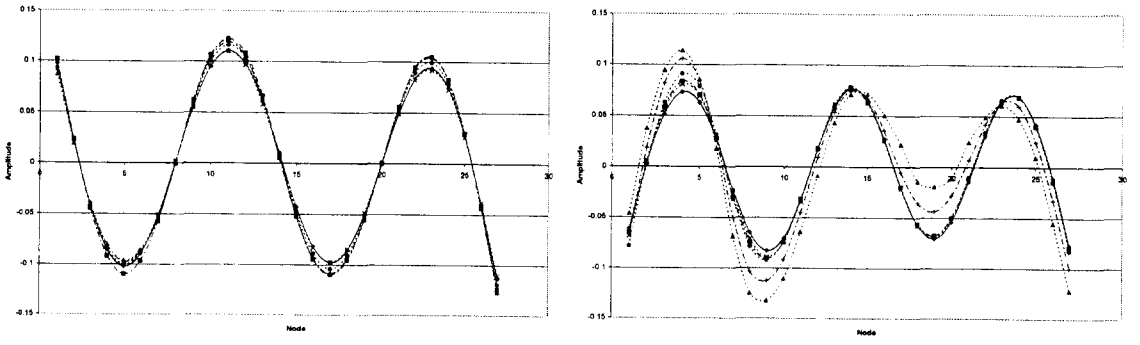

(e) Mode 5 (f) Mode 6

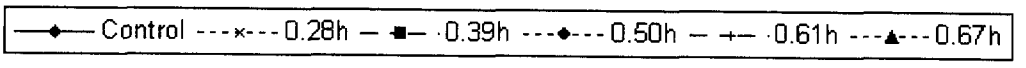

Figure 5.8 First six flexural mode shapes for free-free beam

PERPUSTAKAAN UNIVERSITI MALAYA

Mode 1 Mode 2

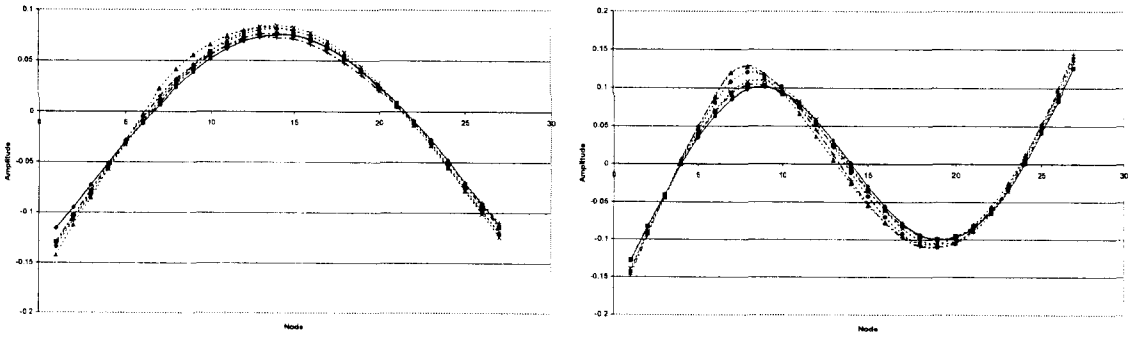

(a) Free-Free

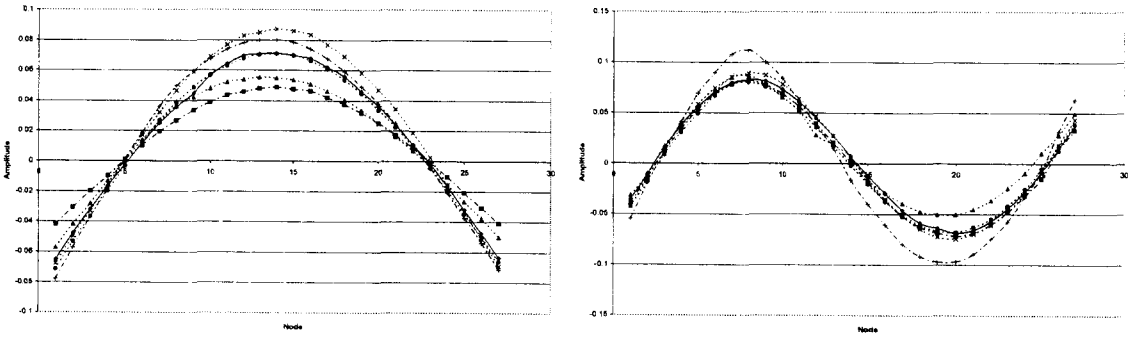

(b) Spring Support

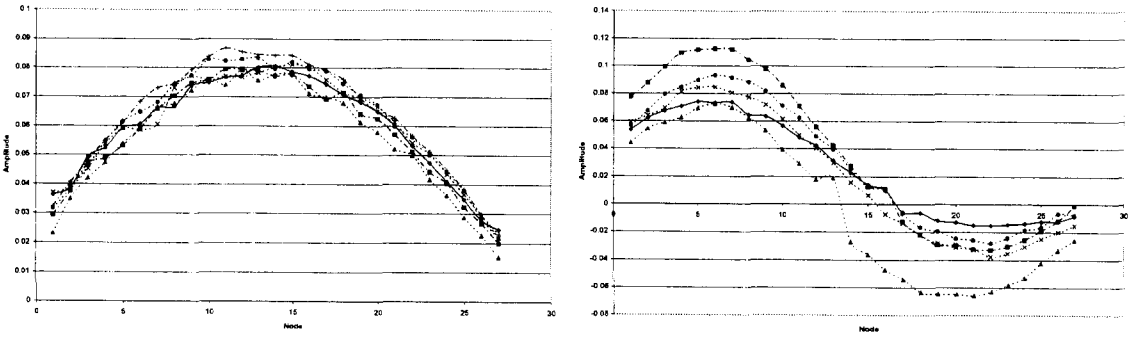

(c) Fixed Roller

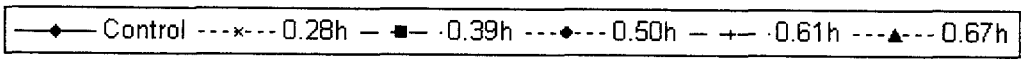

Figure 5.9 Comparison of first two flexural mode shapes in free-free, spring support and fixed roller

5.4.3 CURVATURE MODE SHAPE

Curvature mode shapes are related to the flexural stiffness of a beam [12]. Curvature at a point is given by

$$\kappa = M/(EI) \qquad \text{Equation 5.4}$$

in which κ is the curvature of the section. M is the bending moment at the section. EI is the stiffness of the structure. If a crack or damage occurs in the structure, it reduces the bending stiffness (EI) of the structure at the crack section or in the damaged region, which increases the magnitude of the curvature at that section of the structure. As changes in curvatures are local in nature, they can be used to detect and locate a crack or damage in the structure. Theoretically, the magnitude of changes in curvatures is inversely proportion to the value of EI. Therefore, the state of damage can be obtained from the magnitude of change in curvature.

Ratcliffe [13] successfully developed a technique to detect or identify the location of damage in a beam. When a beam is subjected to localized damage, the mode shape changes and there is also a localized change in curvature mode shape. In modal analysis, the mode shape data are discrete in space, and therefore the changes in slope can be estimated using a central difference approximate on the discrete mode shape. Accordingly, the Laplacian difference equation function is applied to a one-dimensional beam in the following form,

$$L_n = (y_{i+1} + y_{n-1}) - 2y_n \qquad \text{Equation 5.5}$$

L_n – one dimensional Laplacian

y_n – discrete mode shape

The curvature mode shapes using Laplacian equation for the first three flexural modes of the free-free beam with different levels of damage between nodes 7 and 8 are illustrated in Figure 5.10. For mode 1, eventhough the Laplacian exhibited anomalies at

nodes 7 and 8 however other anomalies were also noticeable along the beam. Due to the low complexity of the displacement mode shape for mode 1, the length of the damaged region is relatively short in comparison to the distance between nodes and would not influence the mode shape significantly [28]. Moreover, the existing anomalies can be contributed by the rigid body mode which possibly affected the mode shape data, especially the first flexural mode.

For higher modes such as, in the case of modes 2 and 3, the mode shapes became more complex comprising of more nodes along each flexuring span with each of them far from the influence of the rigid body mode. Consequently, the aspect ratio between the length of damage zone and the distance between nodes would be higher. Hence, the local change in structural stiffness occurring within the damaged zone would affect the mode shape more significantly.

When the cut was greater than 0.5h or 50% damage induced, modes 2 and 3 showed a distinct anomaly at nodes 7 and 8 where the damage was located. It was apparent that the anomaly was sufficient to indicate the damage location without any prior knowledge of a modal test on an undamaged beam. By comparing the undamaged curvature, it was noticed that the higher the degree of the damage, the higher was the change in its curvature. This indicated that the curvature was inversely proportional to the value of structural stiffness and the state of the structure can possibly be estimated from the changes in magnitude in the curvature.

Referring to Figure 5.11, the higher modes were less sensitive to the Laplacian equation where no anomaly was noticeable at the damaged location compared with lower modes when the cut damage was 0.5h. When the cut was 0.61h, the anomaly for the higher modes was not as distinct as that of the lower modes. It was difficult to notice the anomaly at the damage location for the higher modes without comparing it with the undamaged curvature. This indicated that the higher modes were less sensitive and not

applicable for identifying the damage location. However, the higher modes in particular can be used to verify the results from the lower modes.

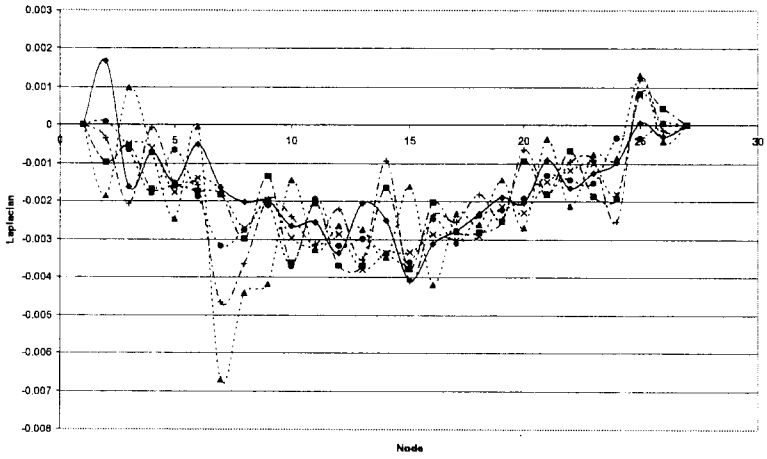

(a) Mode 1

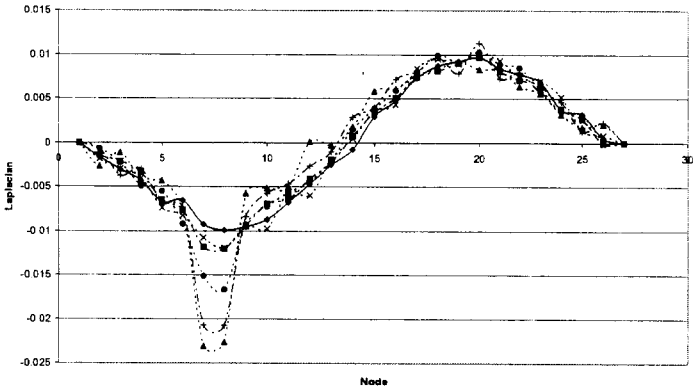

(b) Mode 2

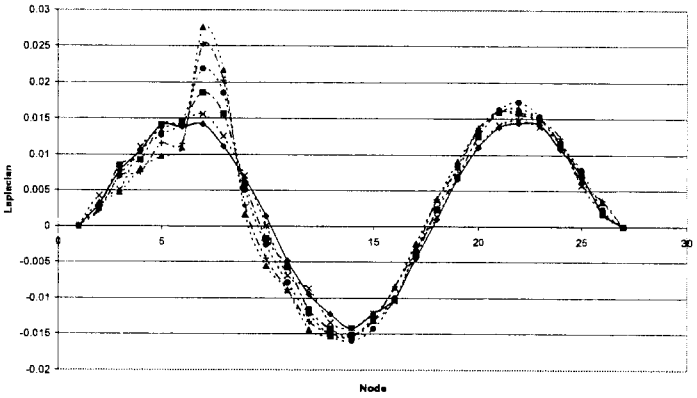

(c) Mode 3

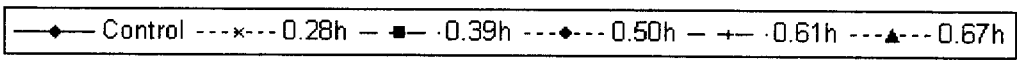

Figure 5.10 Curvature mode shape of free-free beam for first three flexural modes

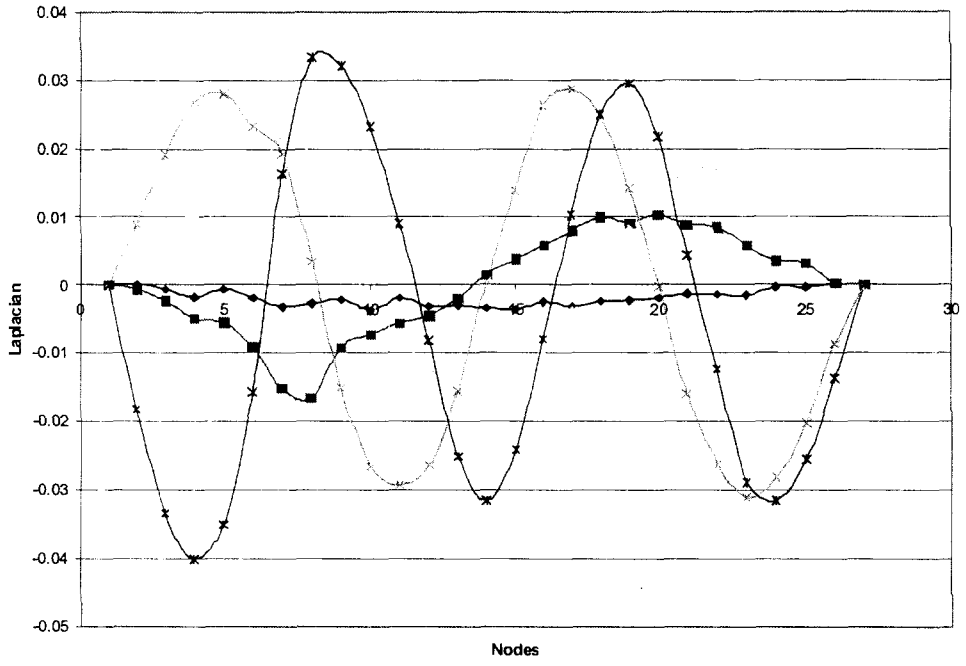

(a) 0.5h cut

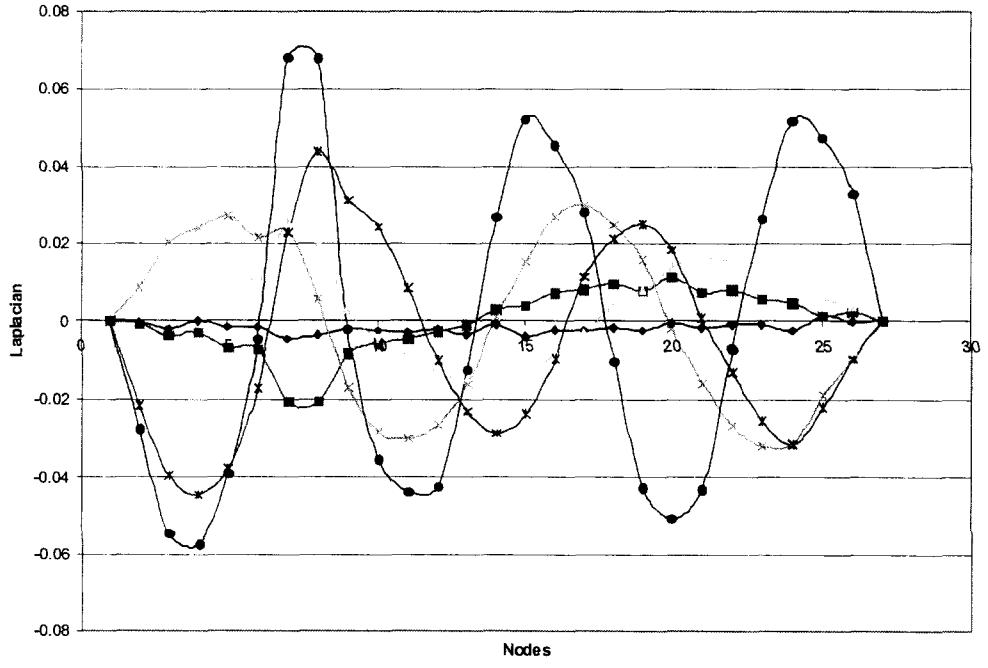

(b) 0.61h cut

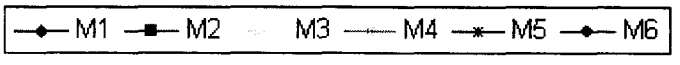

Figure 5.11 Six curvature mode shapes of free-free beam for (a) 0.5h cut and (b) 0.61 cut

Based on previous studies, the experimental curvature mode shape or Laplacian equation was applied to the eigenvector of the free-free beam only [13]. Difficulty to obtain an accurate eigenvector for other boundary conditions was a reason for not using mode shape data as a damage indicator. In this investigation, the curvature mode shapes for the first three flexural modes of the spring and fixed roller supported beams were plotted in Figures 5.12 and 5.13. The curvatures of modes 2 and 3 although presented anomalies at nodes 7 and 8, they were not distinct as other anomalies were also noticeable and they occurred rather arbitrarily at positions other than the damage location. This indicated that as the stiffness of the support condition increased, the mode shape curvatures were affected not only by the damage induced but also by some other factors, especially for the lower modes.

As the mode increased, the mode shape was less affected by the boundary condition, as mentioned in section 5.3.2. In other words, the damage induced became the main source causing the changes in mode shape curvature. However as mentioned earlier, the higher modes were less sensitive and not viable enough as damage indicator by using the Laplacian equation. Thus, it can be deduced that the Laplacian equation as proposed by Ratcliffe was only applicable when the level of damage was fairly severe in the beam with free-free boundary condition for damage location detection. However, it was insufficient for detecting local change in structural stiffness when stiffer boundary conditions were encountered, and thus becomes necessary to use other forms of algorithm.

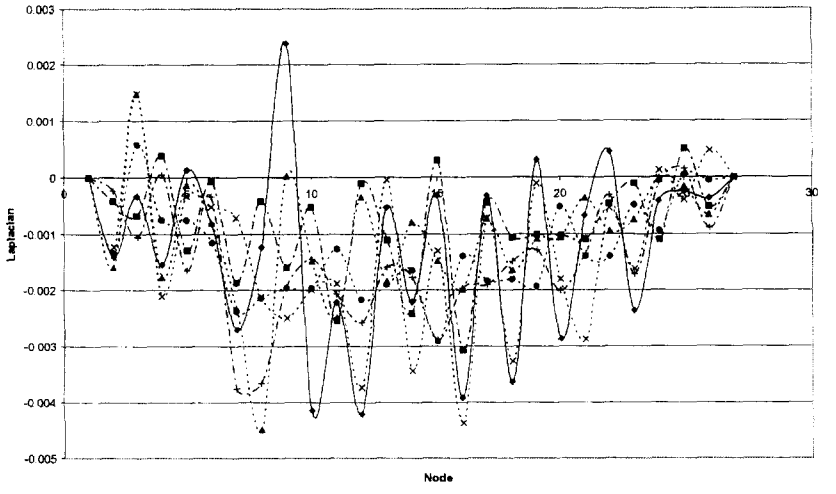

(a) Mode 1

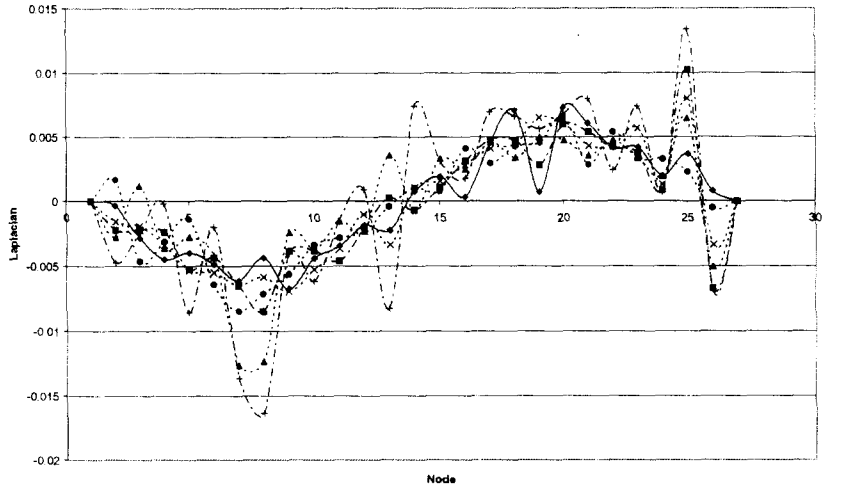

(b) Mode 2

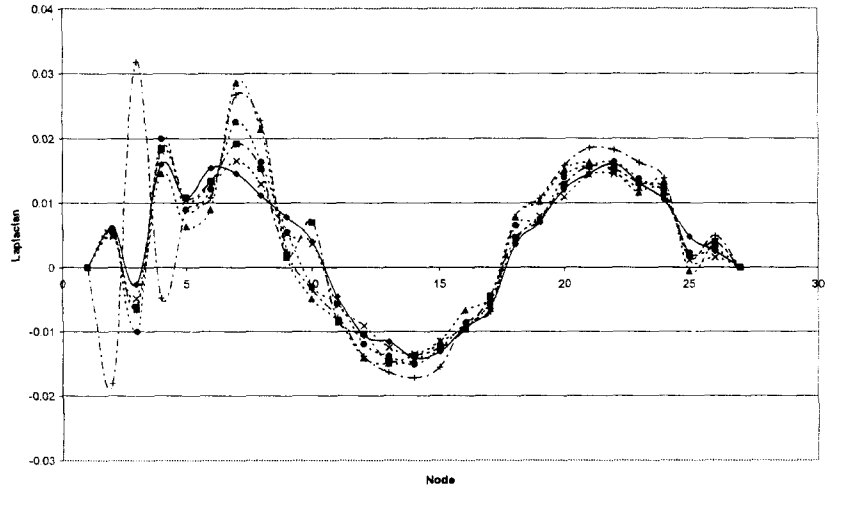

(c) Mode 3

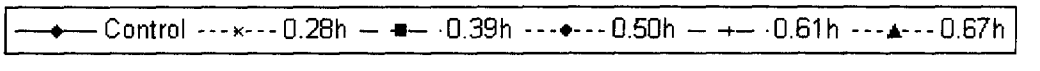

Figure 5.12 Curvature mode shape of spring support beam for first three flexural modes

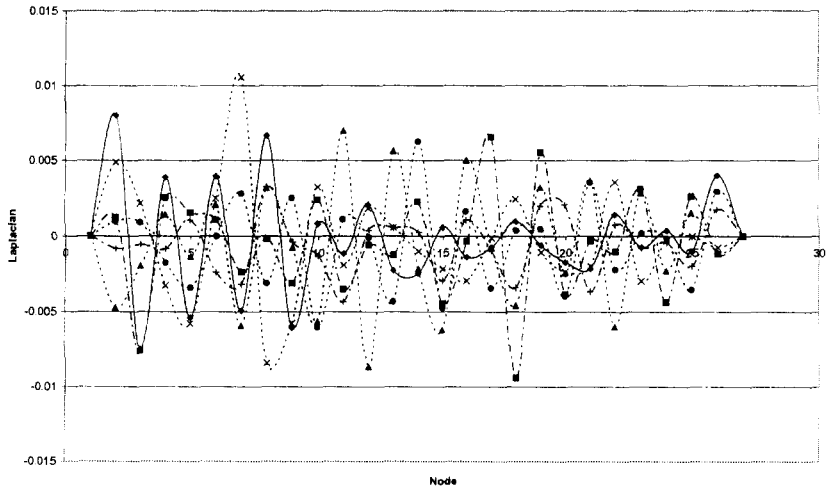

(a) Mode 1

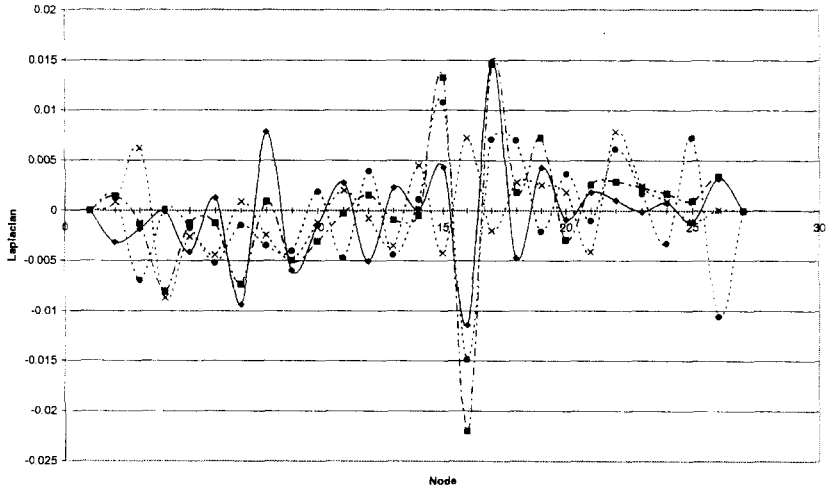

(b) Mode 2

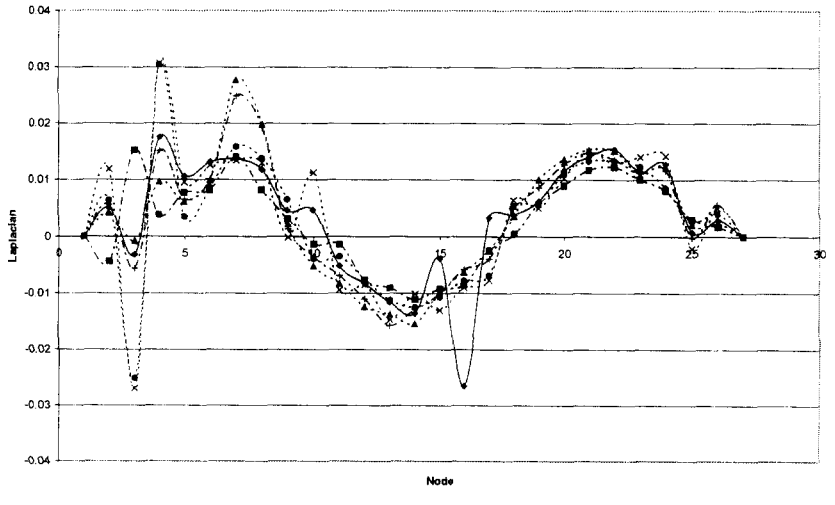

(c) Mode 3

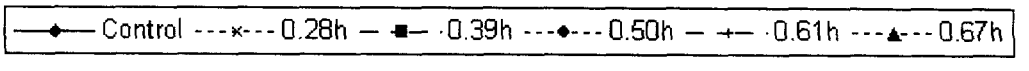

Figure 5.13 Curvature mode shape of fixed roller supported beam for first three flexural modes

5.4.4 COMBINED METHOD

Considering that the Laplacian equation dealt with the deviation of the function value y_n from the arithmetic mean of the neighboring values, its value can thus fluctuate from positive to negative, which makes the detection not sensitive, especially for the higher modes as shown in section 5.4.3. In order to overcome this problem, the geometric mean operator (*GMO*) is proposed to the value of Laplacian. In the mathematical terms, the geometric mean (*Gm*) is defined as:

$$Gm = L_n = \sqrt{L_{n-1} \times L_{n+1}} \qquad \text{Equation 5.6}$$

By modifying the geometric mean, the *GMO* can be written as

$$GMO = L_n - \sqrt{L_{n-1} \times L_{n+1}} \qquad \text{Equation 5.7}$$

or in another form which is

$$GMO = (L_n^2 - (L_{n-1} \times L_{n+1}))^2 \qquad \text{Equation 5.8}$$

where L is the value of the Laplacian at the point, n.

The square is chosen instead of the square root for more efficient calculation of this operator since it deals with the deviation value L_n from the geometric mean of the neighboring values. This operator ensures that the deviation of L_n from the neighboring values is always positive and it will be magnified when there is a deviation due to the change in curvature mode shape. By substituting the value of the Laplacian into Equation 5.8, it is possible to increase the sensitivity of damage detection because of the increasing deviation at the damage location, especially for the higher modes.

For this investigation, the combined method using GMO and Laplacian for free-free, spring and fixed roller support conditions were plotted as illustrated in Figures 5.14, 5.15 and 5.16 for the purpose of comparison. As shown in Section 5.4.3, the support stiffness had less effect on the higher modes but they were less sensitive to the Laplacian equation. So by using the higher modes that is modes 4, 5 and 6, the difference between the Laplacian and the combined method can be clearly noticed.

Referring to Figures 5.14, 5.15 and 5.16, the combined method of all the boundary conditions showed a distinct anomaly at nodes 7 and 8 where the damage is located. Although some anomalies were also noticeable in modes 4 and 5, they were not as distinct as before, in the case of the Laplacian. By comparison, the anomaly for the combined method is clearly noticeable and more distinct than the Laplacian.

In Figure 5.16, mode 6 showed the distinct anomaly at the damage location when the cut was greater than 0.39h. However for the Laplacian, the anomaly at the damage location was only noticeable when the cut was greater than 0.5h as given in Section 5.4.3. Thus it can be deduced that the combined method as proposed is more applicable and sensitive in detecting the damage location than the Laplacian. It is applicable not only for the free-free beam but also for beams with other boundary conditions.

5.4.5 MODAL ASSURANCE CRITERION (MAC)

Modal assurance criterion (MAC) is a technique used to indicate the correlation between two sets of mode shape data using an orthogonality check on the eigenvectors. It is used to study overall differences in the mode shapes. If changes occur in a test structure, there would be modifications to the mode shapes. Thus, the mode shapes before and after the system experience changes are incompatible and their eigenvectors are not perfectly correlated.

Laplacian Combined Method

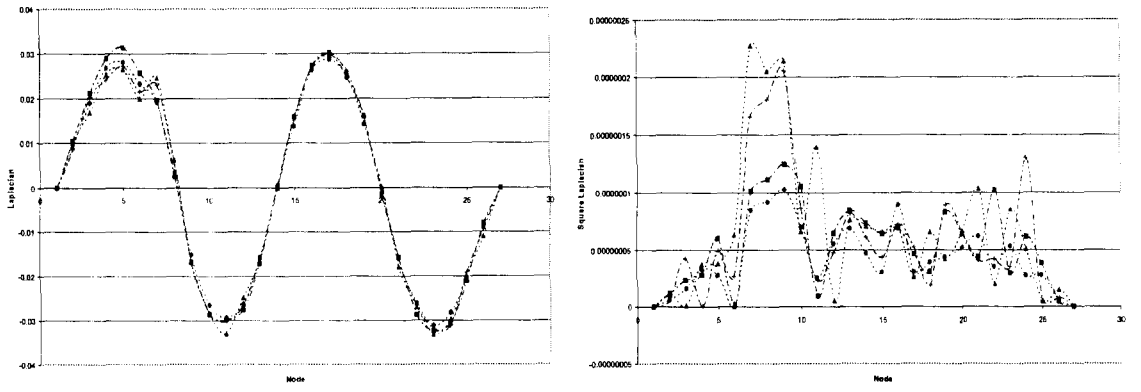

(a) Free-Free

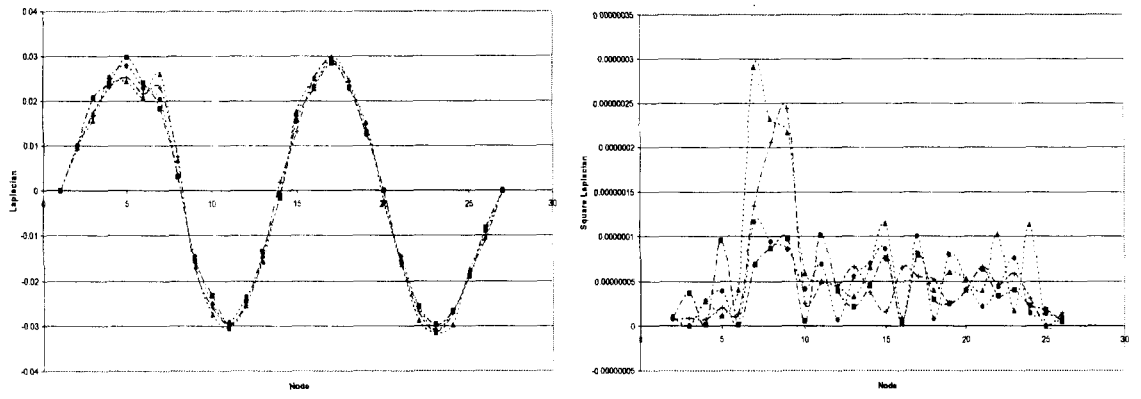

(b) Spring Support

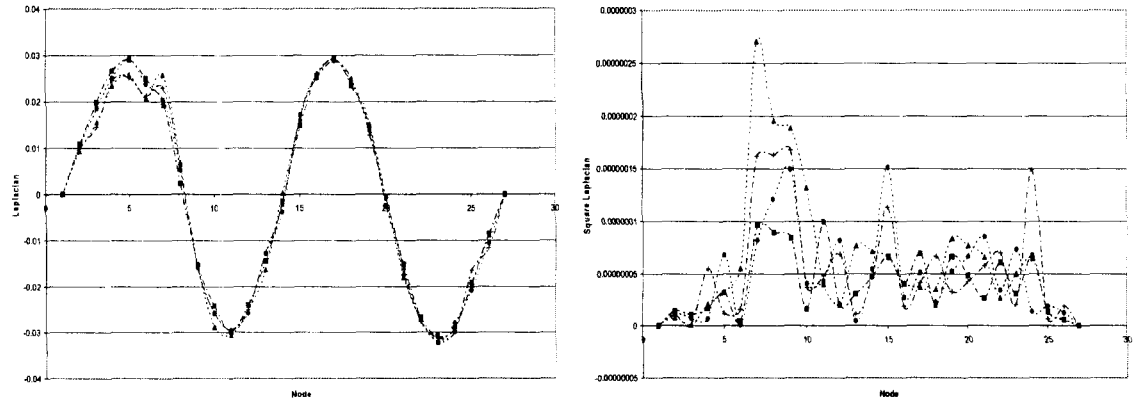

(c) Fixed Roller

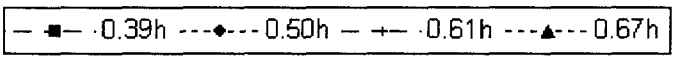

Figure 5.14 Comparison between Laplacian and combined method for flexural mode 4 in (a) free-free, (b) spring and (c) fixed roller support conditions

Laplacian Combined Method

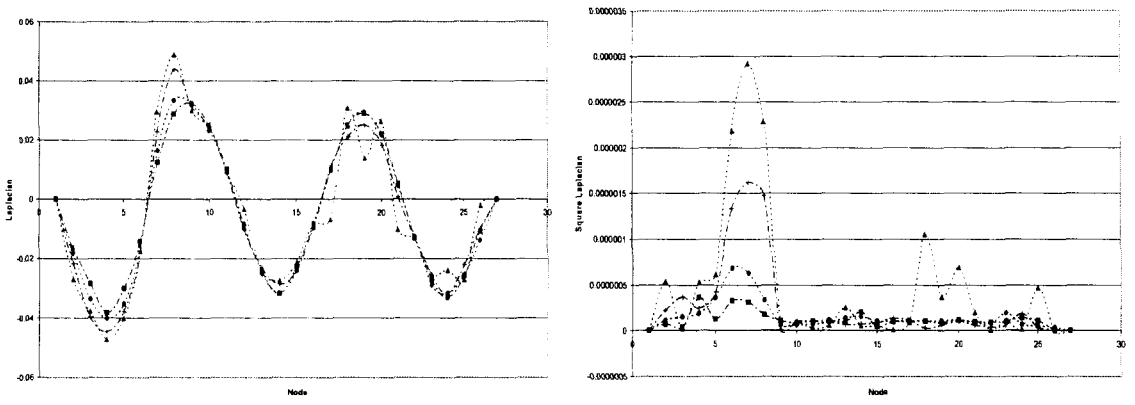

(a) Free-Free

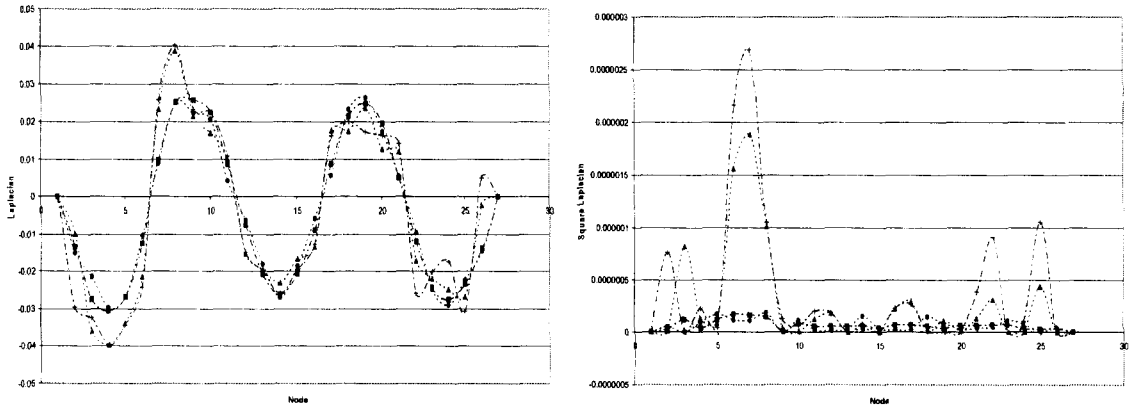

(b) Spring Support

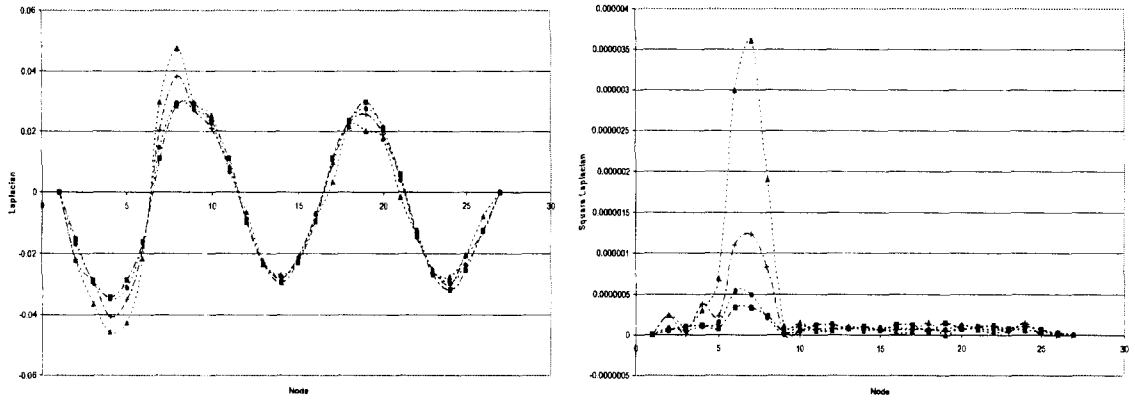

(c) Fixed Roller

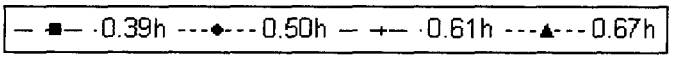

Figure 5.15 Comparison between Laplacian and combined method for flexural mode 5 in (a) free-free, (b) spring and (c) fixed roller support conditions

Laplacian Combined Method

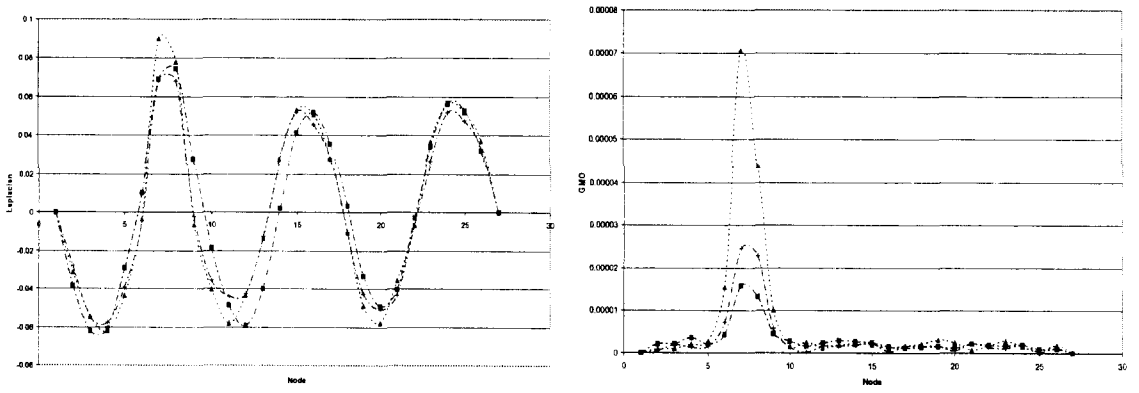

(a) Free-Free

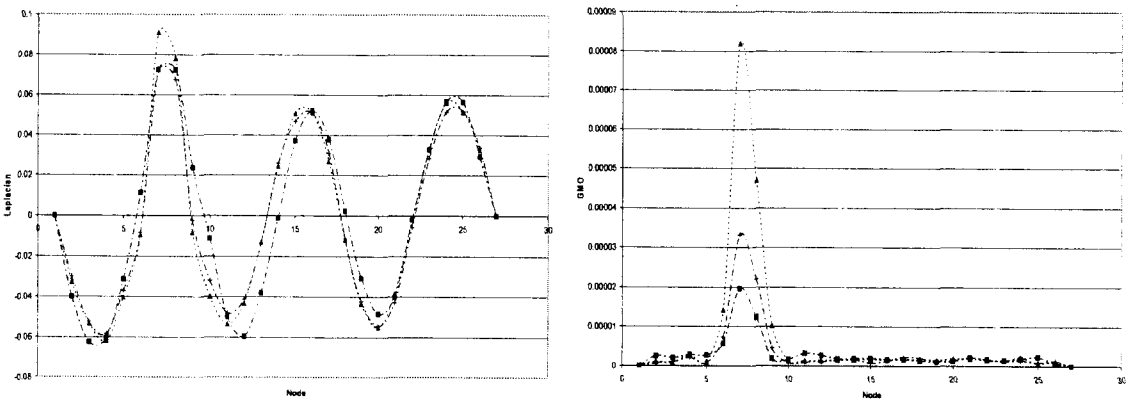

(b) Spring Support

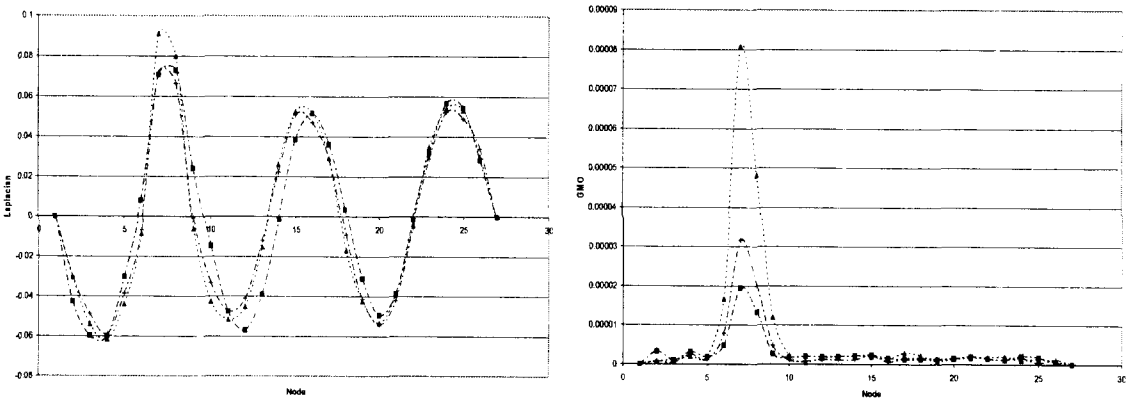

(c) Fixed Roller

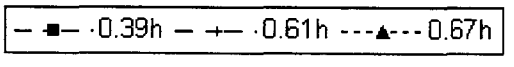

Figure 5.16 Comparison between Laplacian and combined method for flexural mode 6 in (a) free-free, (b) spring and (c) fixed roller support conditions

The MAC between the *q*th mode of the first data set A and the *r*th mode of the second data set B is defined by Allemang and Brown [29] as shown in Equation 5.8. This technique is available to compare two sets of measured data, theoretical versus measured data or two sets of theoretical vibration data. The MAC value indicates the degree of correlation between the two sets of mode shapes. It is therefore possible to infer that the system has experienced changes to its global dynamic parameters. A MAC value close to unity indicates good correlation, while a value close to zero indicates no correlation.

$$\mathrm{MAC}(\{\phi_A\}_q \cdot \{\phi_B\}_r) = \frac{\left|\{\phi_A\}_q^T \{\phi_B\}_r\right|^2}{(\{\phi_A\}_q^T \{\phi_A\}_q)(\{\phi_B\}_r^T \{\phi_B\}_r)} \qquad \text{Equation 5.8}$$

in which $\{\phi_A\}_q$ = mode shape vector for mode q of data set A

$\{\phi_B\}_r$ = mode shape vector for mode r of data set B

Figure 5.17 shows the trend in the MAC values as function of the damage level induced by a saw cut at the soffit of the beam for all the boundary conditions. The real values of the eigenvectors from the first six flexural mode shape data were used to calculate MAC using Equation 5.8. Referring to Figure 5.17, on average the MAC values remained above 0.95 when the cut damage was less than 0.5h for all the boundary conditions. When the cut was greater than 0.61h, only the higher modes, namely modes 5 and 6 exhibited significant drop in MAC values compared to the 0.5h cut. The formation of a plastic hinge significantly affected the mode shape which caused the drop in MAC values.

According to a study conducted by Choi [30], the bending modes of undamaged beams gave MAC values higher than 0.95. Therefore, it was suggested a value of 0.9 for the MAC as an appropriate threshold to indicate changes to the mode shape which were caused by damage induced in the system. This suggested threshold value was to take into consideration human errors and noise during data acquisition, other inaccuracies

during the analysis process, as well as variation between test beams. From this study, the MAC values obtained from the experiment was not sensitive enough to detect any damage in the earlier stages, when the cut was less than 0.5h. This was because the cut was local and affected the eigenvectors near the damage area. However, the MAC value was calculated based on averaging the entire measured eigenvectors, which overshadowed the effect of the damage.

In contrast to the results on natural frequencies as presented earlier in Section 5.4.1, the trends of the MAC values were not consistent. Generally the decreases in MAC values are due to the reduction of the bending stiffness in the beam. However, certain modes presented inconsistent trend when the cut depth was increased as shown in Figure 5.17. The inconsistent trend can be explained by the high sensitivity of the MAC values towards measurement errors [38]. The measurement errors occurring at certain points may significantly influence the MAC values, even though the displacement mode shapes remain the same at other points. This therefore indicated the difficulty of using MAC to evaluate the state of health of a structure.

Based on the above observation, the MAC is not a good damage indicator compared with the drop in natural frequency. The MAC values remained above 0.95 when the cut was less than 0.5h and below 0.9 when the cut was greater than 0.61h, especially for the higher modes. Besides that, the drop in MAC was inconsistent due to the severity of damage. In conclusion, MAC can only indicate the occurrence of severe damage and not suitable to evaluate the overall state of health of a structure.

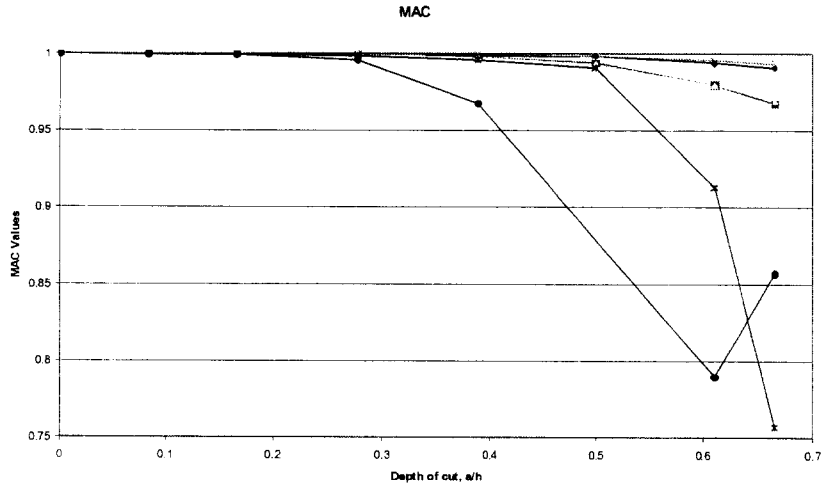

(a) Free-Free

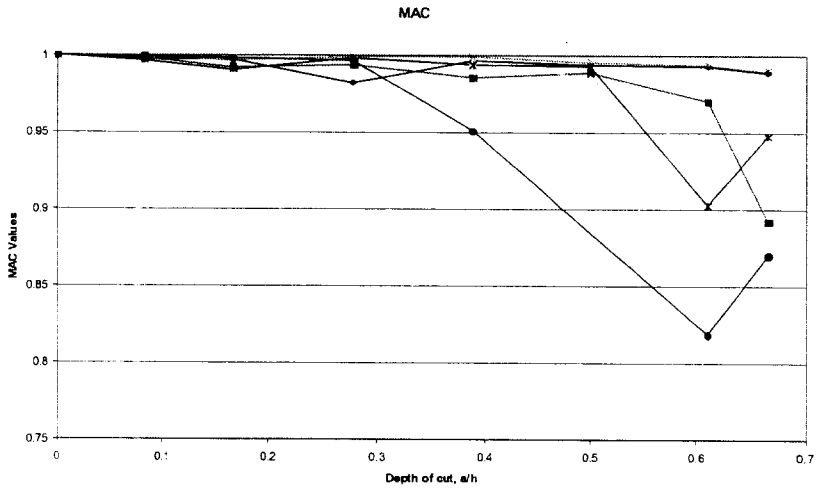

(b) Spring Support

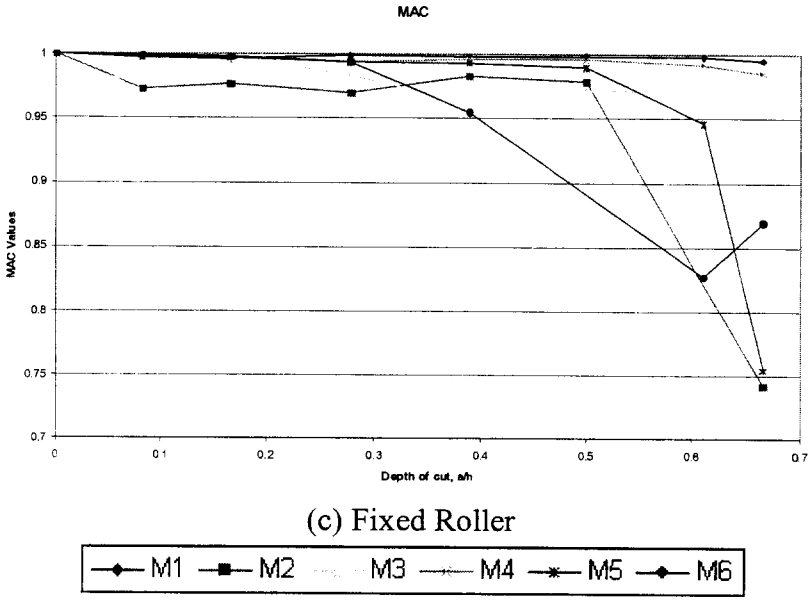

(c) Fixed Roller

Figure 5.17 MAC values in function of damage level for (a) free-free, (b) spring and (c) fixed roller support conditions

5.4.6 COORDINATE MODAL ASSURANCE CRITERION (COMAC)

Coordinate modal assurance criterion (COMAC) is a technique used to indicate the correlation between the mode shapes at a selected measurement point of a structure. It is used to study the differences at every location over the entire mode shape. If local changes occur in a test structure, there would be a modification to the mode shapes. Thus, the displacement mode shapes before and after the system is subjected to damage, experience incompatibilities.

The COMAC for measurement location i is defined by Lieven and Edwins [15] as shown in Equation 5.9. This technique can possibly be use to infer damage locations on the test structure. A COMAC value indicates the degree of correlation at the selected location between the two sets of data. A value close to unity indicates good correlation, and correspondingly a value close to zero indicates no correlation.

$$\mathrm{COMAC}(i) = \frac{\left[\sum ({}_i\phi_A)_l ({}_i\phi_B)_l\right]^2}{\sum ({}_i\phi_A)_l^2 \sum ({}_i\phi_B)_l^2} \qquad \text{Equation 5.9}$$

where i = measurement location

L = total number of correlated mode pairs

$({}_i\phi_A)_l$ = element of mode shape vector for set A in correlated mode pair l

$({}_i\phi_B)_l$ = element of mode shape vector for set B in correlated mode pair l

for which the summation is from $l = 1$ to L.

Figure 5.18 shows the values of subtracting the COMAC value from unity (1-COMAC). The (1-COMAC) values were obtained with varying levels of damage for the beam for all the boundary conditions. The real values from the bending modes were used to calculate the COMAC using Equation 5.9. Although the cut was increased to 0.5h or 50% of damage induced, the (1-COMAC) values remained below 0.05 except the locations near to the support. This indicated that the COMAC is not sensitive to detect the damage at the earlier stage.

When the cut was greater than 0.61h, the drop in COMAC values was distinct, which was over 10% at the damage location for all the boundary conditions. However, the drop not only occurred at the damage location, but also noticeable at other locations. Thus, this showed that the formation of a plastic hinge not only significantly affected the displacement mode shape at the damage location but also affected the other displacement mode shapes. Based on the above result, COMAC is not applicable to indicate the damage location. The drop in COMAC values remained below 5% for low levels of damage. Under more severe condition with the formation of a plastic hinge, the changes in displacement mode shape were global in nature which affected the overall COMAC values.

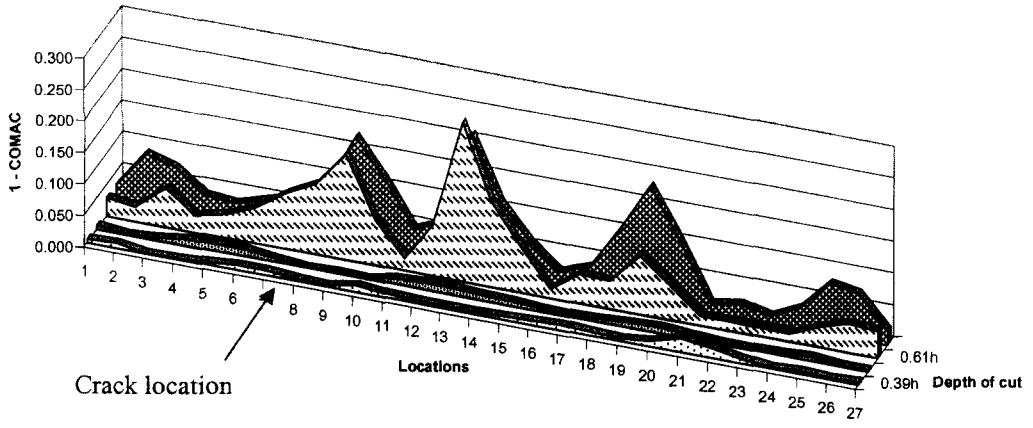

(a) Free-Free

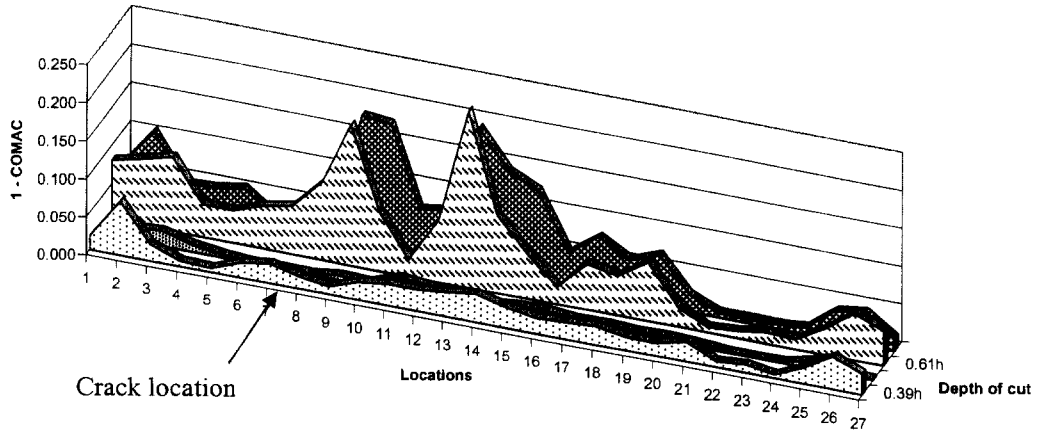

(b) Spring Support

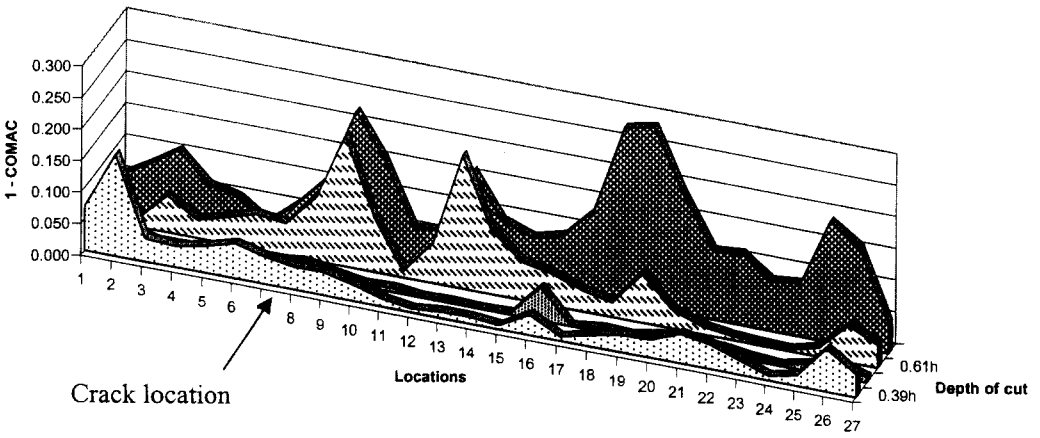

(c) Fixed Roller

Figure 5.18 (1-COMAC) values as function of damage level for (a) free-free, (b) spring and (c) fixed roller support conditions

5.5 DUAL CRACKS

As discussed in Section 5.4, the damage identification techniques were applied to the single crack case. Looking at it practically, the number of cracks present in a structure is usually more than one. As such in this investigation, two saw cuts were introduced at quarter span and mid span points to simulate multiple open cracks at the soffit of the beam. The changes in natural frequencies and the combined method were used to evaluate and detect the crack locations.

Comparisons of percentage drop in natural frequencies between single crack and dual cracks for all the boundary conditions are summarized in Table 5.4. The missing frequencies of the flexural modes in Table 5.4 were due to the identification problems as a result of closely spaced flexural and torsional modes. This was due to the smaller effect of the damage on the torsional mode compared to the flexural mode, which caused the changes in sequence between torsional mode and flexural mode during the damaging process.

As mentioned earlier, the drop in natural frequencies is a function of the damage location. Referring to Table 5.4, it was observed that the second crack induced in the mid span significantly affected the odd modes only. By comparison, the percentage drop in natural frequencies for the odd modes greatly increased compared with the even modes. This indicated that the percentage drop in natural frequencies is a function of the damage locations even though more than one crack occurred in the beam.

As cracks existed at two positions in the structure, the problem of crack size and location becomes more complex and a mathematical model is required. Shifrin [31] successfully used the natural frequencies of a cracked beam to evaluate and detect the damage location by using the mass less rotational spring concept. However using the changes in natural frequency technique indicates one possible crack location as shown in Section 5.4.1.2. It does not provide any information on the number of cracks in the

beam. But the minimum percentage drop in natural frequency gives an indication that the cracks are located at the low curvature areas for a particular mode. Referring to Table 5.4, mode 4 gave the minimum percentage drop, which indicated that the cracks were probably located at 0.0L, 0.28L and 0.5L. Thus it provided some possible indication of the damage location which could be used with other techniques of damage identification.

Since changes in curvature mode shapes are local in nature, cracks occurring in the beam can be identified by the curvature or the combined method. Figure 5.19 shows the plots of mode 5 and mode 6 for all the boundary conditions using the combined method. These two modes were selected because the boundary condition did not significantly affect the displacement mode shape and the change was dominated by the damage induced. Moreover, two modes were sufficient to evaluate and detect the crack locations by using the combined method. The missing modes in these figures were due to the identification problem as a result of closely spaced flexural and torsional modes as mentioned earlier.

Referring to Figure 5.19, the combined method showed distinct anomalies at nodes 7 and 8 and node 14 where the cracks were located. However, these two distinct anomalies were not noticeable in the same mode, which appeared separately in the two modes. Mode 5 presented the anomaly at node 14 while mode 6 presented the anomaly at nodes 7 and 8. The distinct anomalies in mode 5 and 6 were due to the magnitude of change in mode shape curvature. As cracks were located at the high curvature zones, the changes in magnitude in curvature mode shape were higher compared to the changes for the crack located at low curvature zone. Although the anomalies were presented in every mode, it was dominated by the crack at the high curvature zone. Hence, the combination of the two modes can still successfully indicate the number of cracks and the crack locations.

Boundary condition	Depth of cut / Modes	1		2		3		4		5		6	
		Single crack	Dual cracks	Single crack	Dual cracks	Single crack	Dual cracks	Single crack	Dual cracks	Single crack	Dual cracks	Single crack	Dual cracks
		Percentage drop in natural frequencies, %											
FF	0.17h	0.33	0.75	0.52	0.57	0.43	0.88	0.06	0.06	0.14	0.54	0.49	0.50
	0.28h	0.67	2.07	1.37	1.39	1.08	2.31	0.14	0.12	0.35	1.50	1.25	1.20
	0.39h	1.08	4.52	3.10	3.03	2.33	4.75	0.25	0.28	0.69	2.97	2.52	2.55
	0.50h	2.28	9.22	5.87	5.39	4.06	8.13	0.47	0.39	1.27	4.92	-	-
	0.61h	4.46	15.83	10.57	10.16	6.75	13.93	0.76	0.73	2.24	8.02	7.50	8.44
SS	0.17h	0.52	2.41	-0.15	0.85	-0.10	0.98	-0.12	0.03	0.04	0.44	0.43	0.48
	0.28h	0.33	2.06	1.43	1.48	0.53	2.67	-0.01	0.28	-1.52	1.58	1.16	1.25
	0.39h	1.01	5.21	3.23	3.58	2.91	5.06	0.35	0.43	0.70	-	2.52	2.53
	0.50h	1.71	7.06	4.03	3.46	3.72	4.84	0.48	0.14	1.05	-	-	0.00
	0.61h	3.58	12.67	8.32	8.30	6.43	11.99	0.86	0.92	2.44	9.01	7.43	8.40
FR	0.17h	-2.12	0.30	0.70	-0.15	0.89	1.82	0.04	0.10	0.11	0.54	0.48	0.51
	0.28h	-0.52	1.05	2.48	1.16	1.99	3.46	0.31	0.13	0.36	1.44	1.23	1.20
	0.39h	-1.24	1.21	0.04	-0.96	2.14	5.11	0.29	0.19	0.64	-	2.50	2.51
	0.50h	-0.06	2.97	2.67	-	3.52	7.74	0.60	0.35	1.19	4.75	-	4.78
	0.61h	2.33	10.07	-	2.76	9.29	13.60	0.97	1.16	2.12	7.97	7.43	8.50

Degree of support stiffness (increase) →

Table 5.4 Comparison of percentage drop in natural frequencies for single crack and double cracks

In conclusion, the combined method is not only applicable for the single crack case but also applicable for the dual crack case. By using the higher modes, the combined method was able to detect local changes in structural stiffness although problems with the stiffer boundary conditions were encountered. The other modes can also be use to verify the results. Moreover by combining the information of changes in natural frequencies, it was evident that nodes 7 and 8 and node 14 were the exact crack locations for the beam.

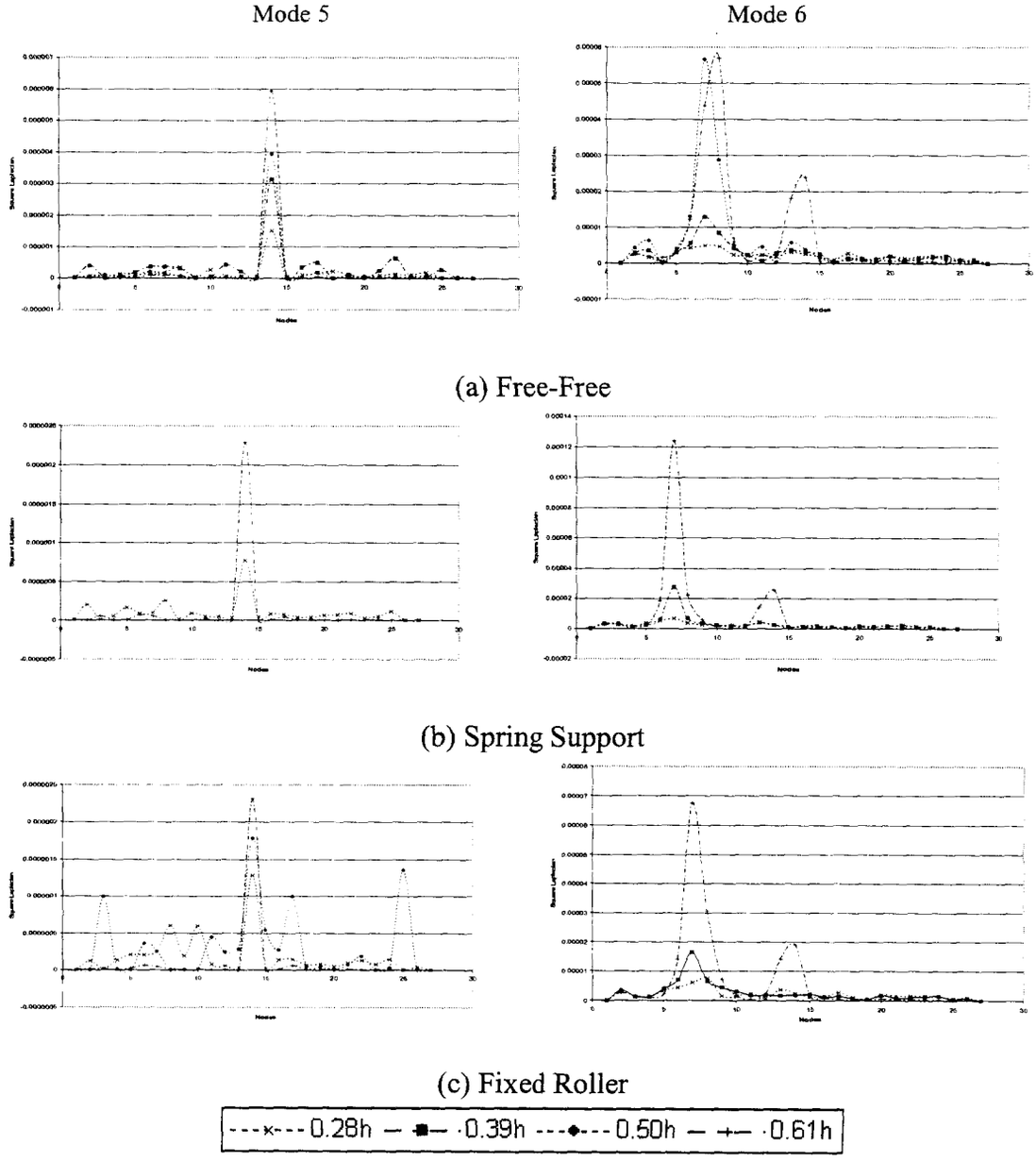

Figure 5.19 The plots of combined method for mode 5 and mode 6 for the (a) free-free, (b) spring and (c) fixed roller support conditions

5.6 MODEL UPDATING

The analytical method namely the finite element (FE) has been developed in the last few decades. As discussed by Mottershead and Friswell [33], the objective of the analytical method is to predict the behavior of a structure and to optimize the design solution. However, the application of the analytical model has some weaknesses i.e. modeling errors and accuracy problems which lead to poor correlation with experimental data. This can provide serious misinterpretation of the analytical results. Therefore the validation of analytical results with the experimental data should be verified at the very beginning of the design process.

5.6.1 COMPARISON OF EXPERIMENT AND PREDICTION

Comparison of experiment and prediction using modal data (natural frequencies and mode shapes) is a common technique used to validate the analytical model. Generally, if two sets of modal data are similar and in agreement with each other then it can be concluded that the analytical model is valid. In this investigation, the measured and the predicted natural frequencies are compared to evaluate the correlation between the two sets of results. This is often done by a simple tabulation of the two sets of results but there is no guarantee that the measured modes are correlated with their predicted data. Therefore positive identification of each mode with its counterpart is essential for providing a set of correlated mode pairs (CMPs). Modal assurance criterion (MAC) is used extensively in the modal analysis community for measuring model similarity and establishing CMPs.

The comparison of the experimental data and FE results for the flexural and torsional modes in free-free and fixed roller supported beams are summarized in Table 5.5 and 5.6. In the FE modeling, the free-free results are likely to provide the information on the inertia properties of the beam for modeling other boundary

conditions. For modeling the support condition, the support properties are important factors for modeling the exact boundary condition. In this investigation, the fixed roller support has some flexibility in the z-axis. When the beam is under vibration, there is the movement up in z direction. Therefore, a spring with a high stiffness value was used to model the fixed roller support.

A similar study was reported by Mottershead [35], who carried out vibration measurements on a cantilever plate with welded joints at the clamped end. The cantilever was updated using the effective length of the element closest to the clamped end or alternatively was modeled with the clamped end as an elastic foundation. The elastic foundation was modeled as a pinned boundary with a rotational stiffness.

Referring to Table 5.5 and 5.6, the FE results of all the first six flexural and torsional modes of the undamaged beams presented good correlation with the experiment data for the both boundary conditions. The overall percentage difference in natural frequencies is below 4% which indicated good correlation except for the first three lower modes of the fixed roller support. Updating the boundary conditions with the elastic support at the edge is not sufficient and ideally, other parameters have to be considered for updating purposes. According to Mottershead[35], the geometric parameters have considerable potential in updating the model. They have physical meaning and the measurements are sensitive to changes in them.

According to Ewins [34], a MAC value in excess of 0.9 should be attained for well correlated modes. From Table 5.5 and 5.6, it was noticed that the MAC values were above 0.9 for every mode pair. This indicated that the mode shape data of FE were correlated with the mode shape data obtained experimentally. The MAC value for the second bending mode for beam 1 with the fixed roller support was much lower comparatively, due to the quality of the modal data. Thus, the FE model were

considered well correlated with the experimental model. The modal data obtained from FE model can be regarded as the data obtained from the experiment.

Modes	Average frequencies of B1 & B2	Frequencies from FEM	Frequencies differences, %	MAC values	
				B1 vs FE	B2 vs FE
M1	83.46	82.69	0.93	0.995	0.994
M2	229.36	230.40	-0.45	0.985	0.981
T1	349.81	358.06	-2.36	0.997	0.999
M3	449.93	456.17	-1.39	0.974	0.971
T2	707.43	724.90	-2.47	0.993	0.994
M4	743.79	754.91	-1.49	0.961	0.957
T3	1083.49	1108.80	-2.34	0.983	0.985
M5	1109.65	1109.50	0.01	0.944	0.948
T4	1482.62	1517.20	-2.33	0.975	0.977
M6	1543.90	1489.30	3.54	0.950	0.945
T5	1913.20	1956.60	-2.27	0.965	0.961

Table 5.5 Comparison of natural frequencies and MAC values for the free-free beams

Modes	Average frequencies of B1 & B2	Frequencies from FEM	Frequencies differences, %	MAC values	
				B1 vs FE	B2 vs FE
M1	31.22	33.80	-8.2	0.984	0.979
M2	130.74	108.60	16.9	0.763	0.935
T1	378.59	407.47	-7.6	0.996	0.996
M3	483.08	487.26	-0.9	0.990	0.975
T2	724.78	753.48	-4.0	0.999	0.992
M4	760.01	771.51	-1.5	0.995	0.964
T3	1096.61	1129.60	-3.0	0.997	0.988
M5	1119.06	1118.80	0.0	0.988	0.975
T4	1494.15	1534.10	-2.7	0.994	0.994
M6	1550.63	1494.40	3.6	0.985	0.986
T5	1921.13	1971.10	-2.6	0.996	0.996

Table 5.6 Comparison of natural frequencies and MAC values for the fixed roller supported beams

5.6.2 CRACK IDENTIFICATION TECHNIQUE

As discussed in Section 5.4.1, the higher the degree of damage in the cracked beam, the higher the change in its natural frequencies. However it was also observed

that for the same level of damage, the change in natural frequencies differed for every mode. Thus, it was inferred that change in natural frequency was affected not only by the crack depth but also by the crack location. Consequently, a particular frequency corresponded to different crack locations and crack depths.

Figure 5.20 and 5.21 illustrate the changes in natural frequencies due to the crack location and crack depth of the first six FE flexural natural frequencies for free-free and fixed roller supported beams. The changes in natural frequencies were obtained by a reducing the flexural stiffness in a particular element. This was supposed to model the stiffness change due to the presence of a crack. The depth of crack was related to the extent of reduction in the flexural stiffness i.e. EI_D/EI. Table 5.7 shows the values corresponding to the level of crack depths.

Normalized EI values for damaged element, EI_D/EI	0.92	0.79	0.58	0.36	0.22	0.12
Corresponding depth of crack	0.06h	0.17h	0.28h	0.39h	0.50h	0.61h

Table 5.7 Degree of damage in FE modeling

Referring to Figure 5.20 and 5.21, the percentage changes in natural frequencies increased when the EI value of the damaged element was reduced in the model. It was also observed that the percentage changes in natural frequencies were different for different crack locations for the same damage level. Mode 1 gave the maximum percentage change when the crack was located at the mid span and the minimum when the crack was at the edge. In other words, the maximum percentage change was located at a high curvature zone and the minimum at the low curvature zone, as shown in Figure 5.22. Similar results were also observed from the other flexural modes. This indicated that the change in natural frequencies is a function of the crack depth and crack location.

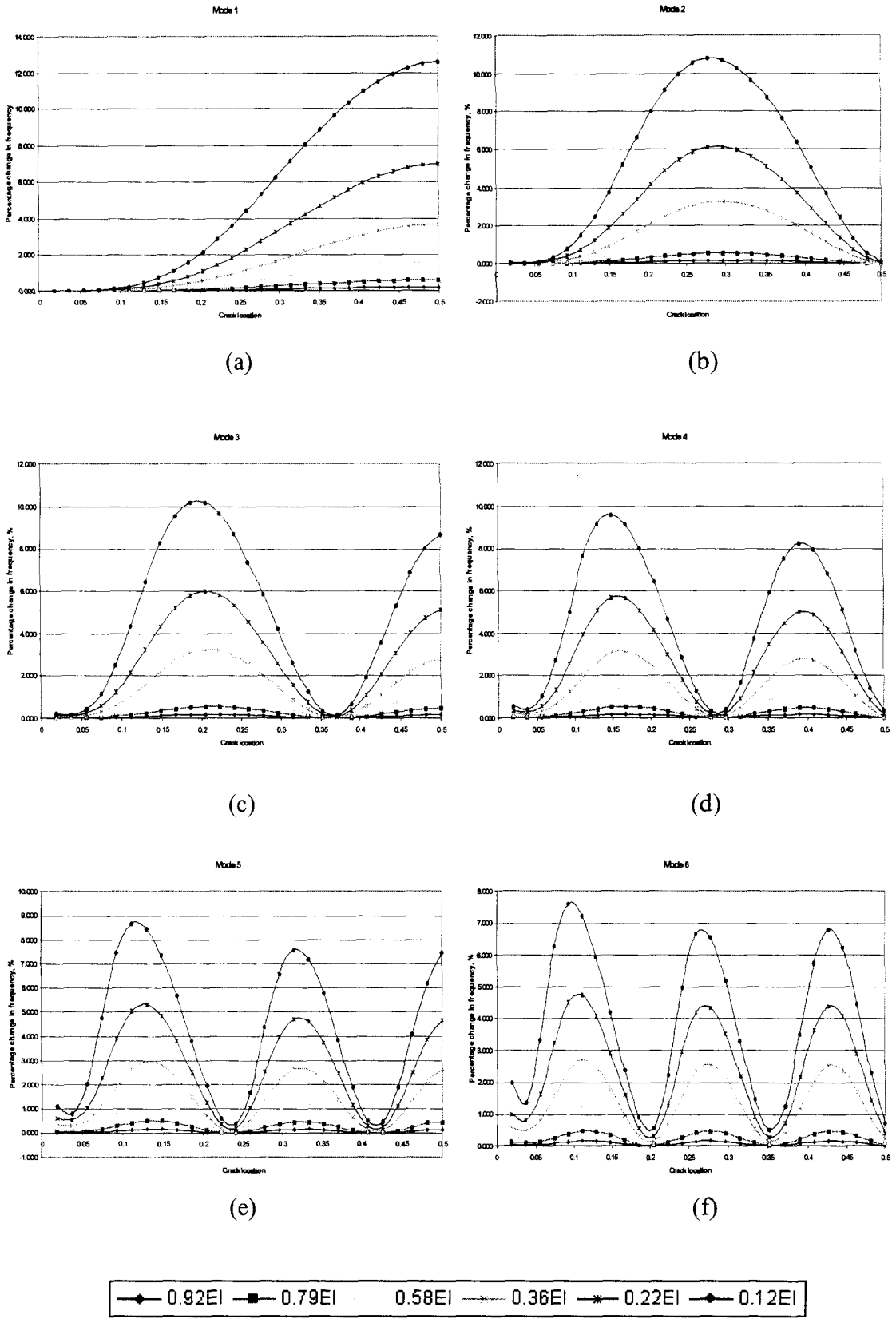

Figure 5.20 Percentage change in natural frequencies due to damaged element in free-free beam

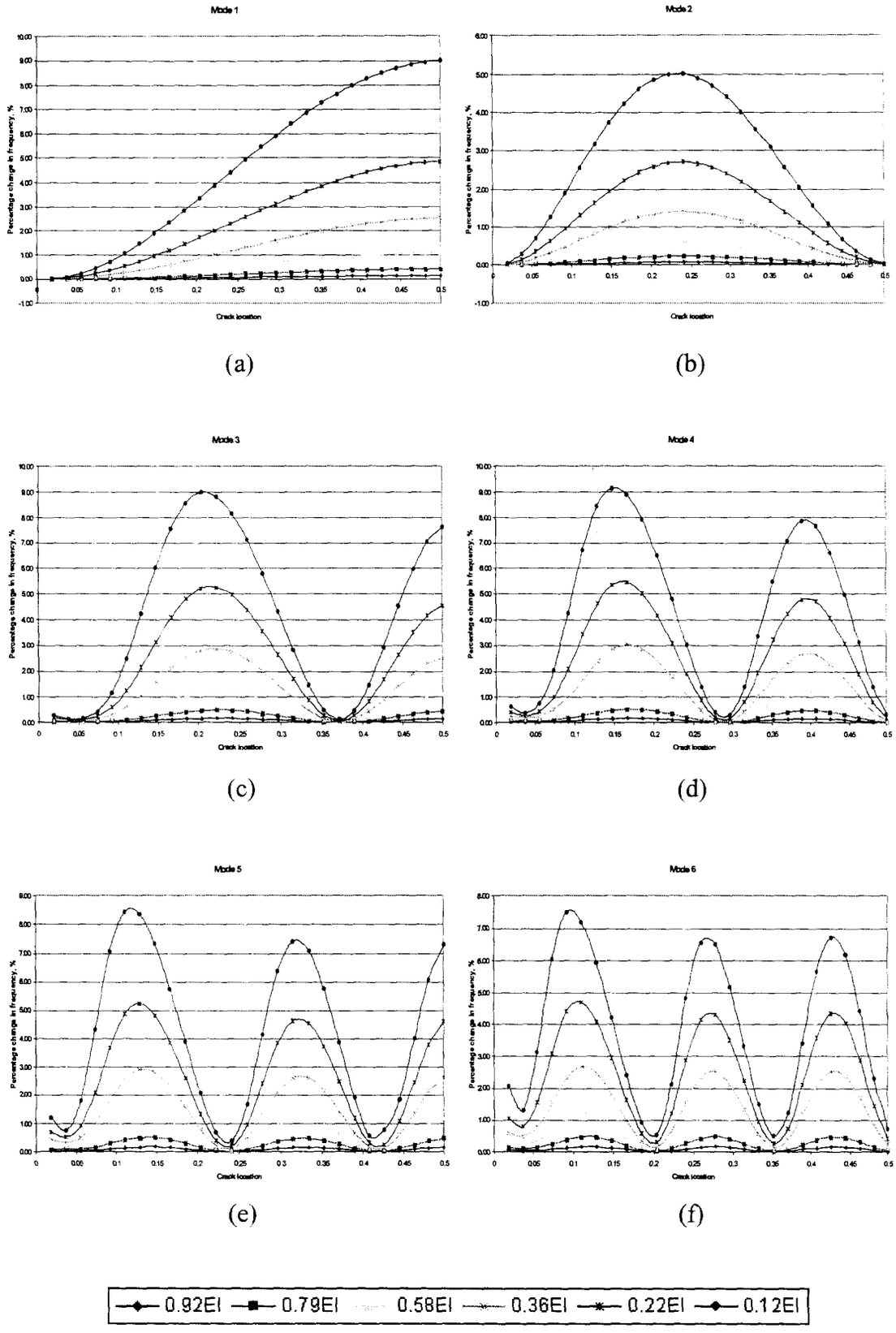

Figure 5.21 Percentage change in natural frequencies due to damaged element in fixed roller supported beam

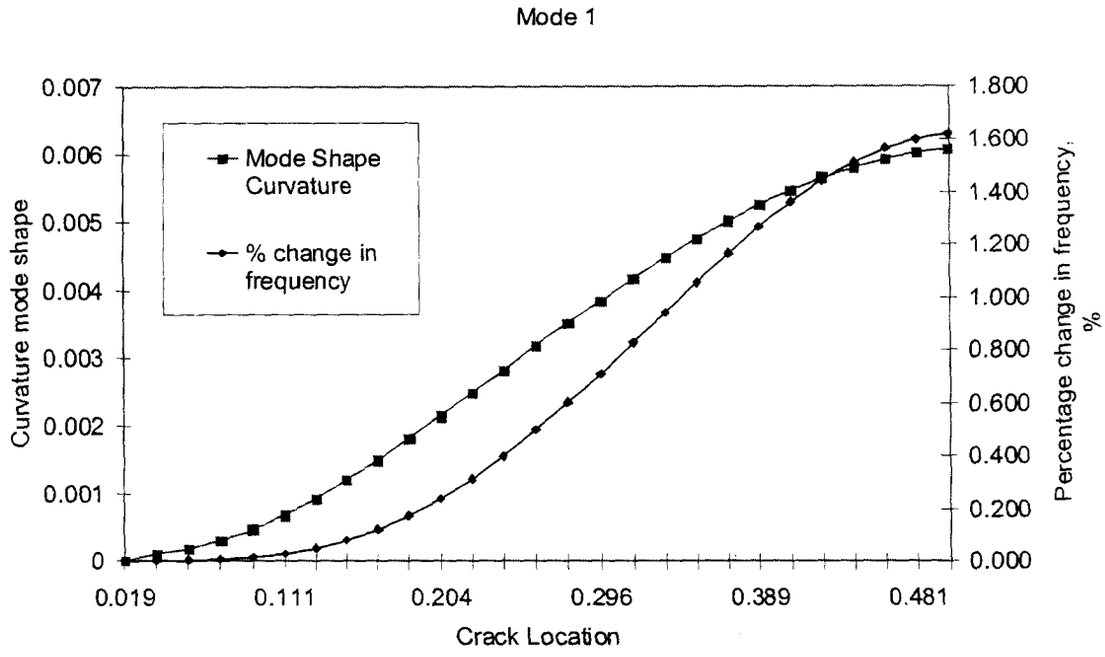

Figure 5.22 Change in natural frequencies due to the damaged element (flexural stiffness = 0.58*EI*) for flexural mode 1

Based on the concept of changes in natural frequencies as a function of the crack location and crack depth, a graph with the same normalized frequency resulting from a combination of different crack locations and crack depths for a particular flexural mode was plotted. It was assumed that the crack depth or normalized *EI* must be the same at the crack location for all the vibration modes. Consequently, by plotting the normalized *EI* along the length of the beam for distinct normalized frequencies, the location of crack and severity of damage can be identified by the intersection of the curves.

In the procedure of identifying the crack location and severity of damage for a single crack case, several steps are required in order to achieve the goal.

1. Measure the first six flexural natural frequencies. Usually three natural frequencies are enough for damage identification but six natural frequencies are recommended in order to improve the statistics of the curve intersection.
2. Normalize the measured natural frequencies, i.e. ratio of $f_{damaged}/f_{undamaged}$.

3. Plot graph (normalized EI versus crack location for constant normalized frequencies) from the different modes on the same axes using the data generated from the FE model (see Appendix A).
4. The intersection point of the different plots indicates the crack location and severity of damage.

This concept was originally proposed by Owolabi [36] for identifying the crack location and crack depth using experimental data while in this study the FE data were used for the same purpose.

From the result of single cracked free-free beam, the normalized frequencies of first six flexural modes obtained from experiment were 0.9967, 0.9948, 0.9957, 0.9994, 0.9986 and 0.9951 for 0.17h cut and 0.9933, 0.9863, 0.9892, 0.9986, 0.9965 and 0.9875 for 0.28h cut. These normalized frequencies were plotted on the same axes as shown in Figure 5.23. From this figure, it was observed that all the lines intersected each other at the relative crack location 0.26 where the crack was located. The approximate values of flexural stiffness, *EI* at the crack location were 0.79EI and 0.58EI which corresponded exactly to 0.17h and 0.28h cut for the beam.

A similar procedure was also applied to a fixed roller supported beam for the cases of 0.17h and 0.28h cut located at the quarter span. Mode 1 and mode 2 were omitted because of the inconsistent change in natural frequencies due to the level of damage, as shown in Table 5.2. This is because the changes in natural frequencies are significantly influenced by the boundary condition, especially for the lower modes.

The normalized frequencies obtained from the experiment for mode 3, mode 4 mode 5 and mode 6 were 0.9911, 0.9996, 0.9989 and 0.9952 respectively for 0.17h cut and 0.9801, 0.9969, 0.9964 and 0.9877 respectively for 0.28h cut. Referring to Figure 5.24, the graphs plotted on the same axes for both crack cases do not show any significant pattern for identifying the crack location and severity of damage. A possible

reason is that for fixed roller supported beam, it is difficult to measure the natural frequencies accurately due to the influence of the boundary condition. The incompatibility of FE results and the experimental data can be another possible reason. However, based on the assumption that the normalized *EI* must be the same at the crack location for all the vibration modes, it can be inferred that the difference of the normalized *EI* values between the modes is small at the crack location. Thus, by subtracting the maximum normalized *EI* and the minimum normalized *EI* will return a minimum value at the crack location.

By plotting the values of the difference in normalized *EI* along the length of the beam, it can be noticed that the minimum value was located at the location 0.26 where the crack was located for both cases, as shown in Figure 5.25. The severity of the damage can be indicated by taking the average values of normalized *EI* which were 0.795EI and 0.487EI for the 0.17h and 0.28h cut respectively.

Based on the above results, a modification of the technique proposed by Owolabi [36] has successfully identified the crack location and severity of damage for the free-free and fixed roller supported beam. However there is a problem for structures with symmetrical mode shapes which possibly presents two crack locations. Thus it is more applicable for the structure with non-symmetrical mode shapes. According to Owolabi [36], in a situation where the crack location coincides with a vibration node, break in the graph was occurred, and no point of intersection can be obtained. However in this investigation, by using the FE data, the graph could be plotted along the beam length and the intersection was always obtained although the crack was located at the vibration node. Moreover sets of experimental data for different crack locations are not required, because these data can be obtained form the FE model. However, it must be emphasized that the FE model must be well correlated with the experimental results. If the correlation is unsatisfactory, then the FE data are not valid for this purpose.

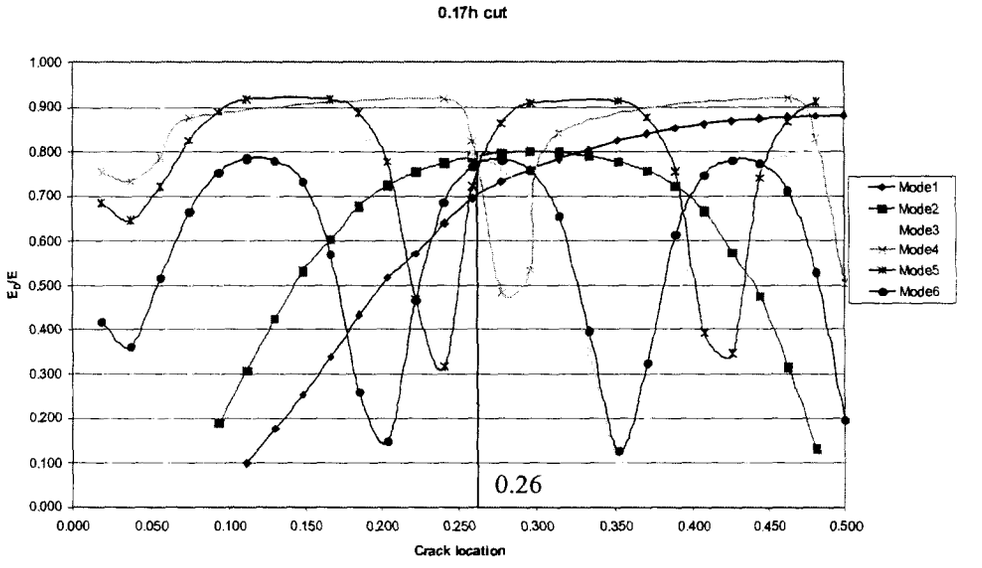

(a) Normalized frequencies for first six flexural modes are 0.9967, 0.9948, 0.9957, 0.9994, 0.9986 and 0.9951 respectively

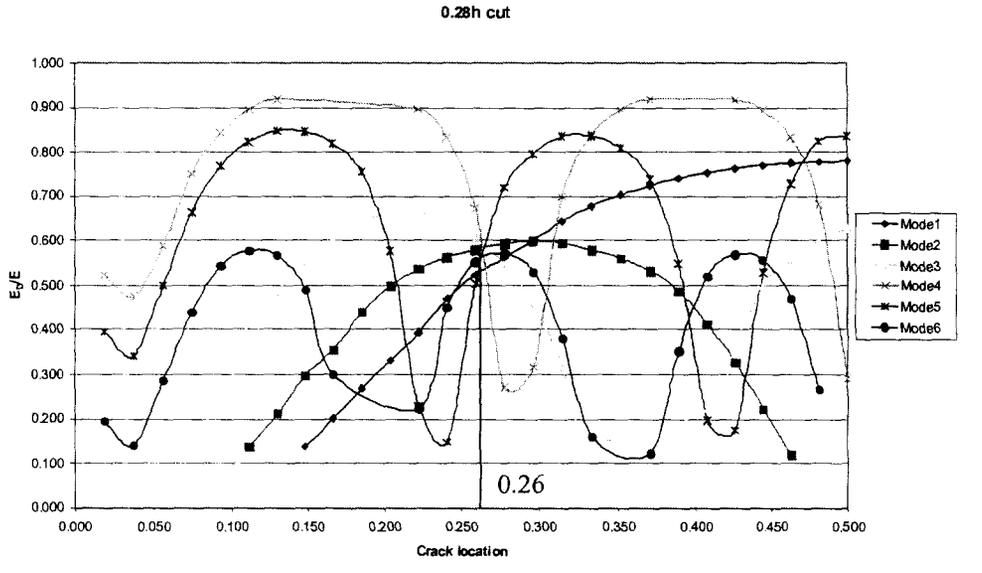

(b) Normalized frequencies for first six flexural modes are 0.9933, 0.9863, 0.9892, 0.9986, 0.9965 and 0.9875 respectively

Figure 5.23 Normalized *EI* versus crack location with the same normalized frequency for the first 6 flexural modes in the free-free beam, (a) 0.17h cut and (b) 0.28h cut

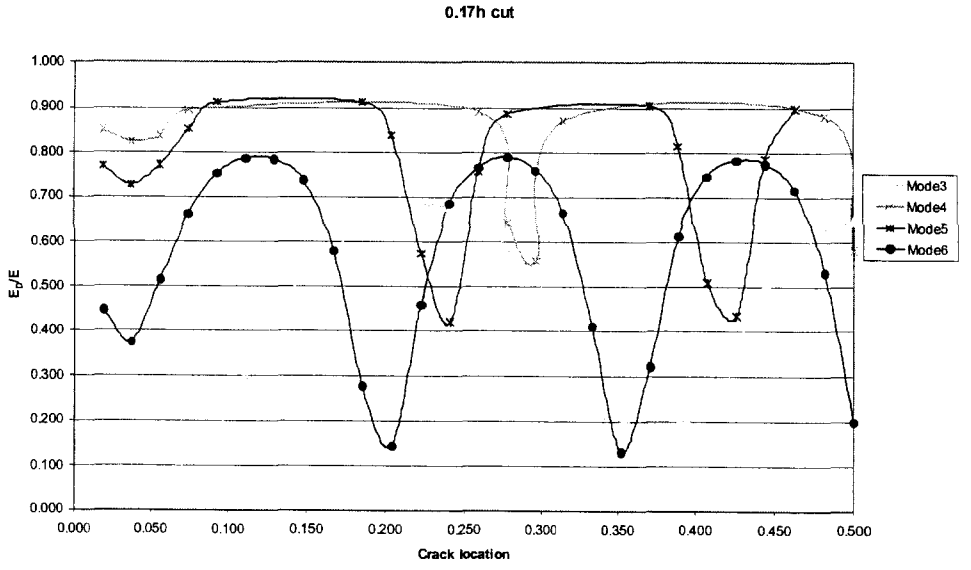

(a) Normalized frequencies for mode 3, mode 4, mode5 and mode 6 are 0.9911, 0.9996, 0.9989 and 0.9952 respectively

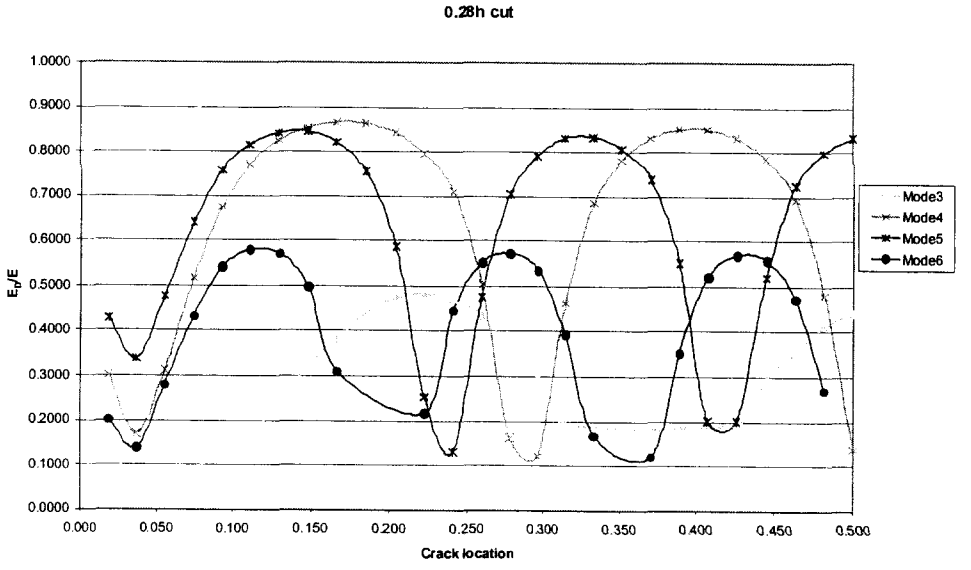

(b) Normalized frequencies for mode 3, mode 4, mode 5 and mode 6 are 0.9801, 0.9969, 0.9964 and 0.9877 respectively

Figure 5.24 Normalized *EI* value versus crack location with the same normalized frequency for the flexural modes in the roller supported beam, (a) 0.17h cut and (b) 0.28h cut

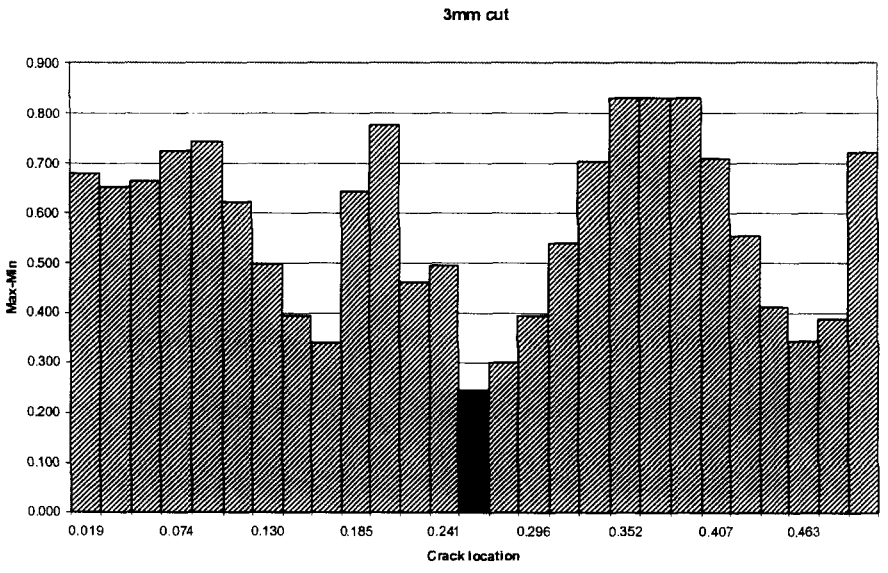

(a)

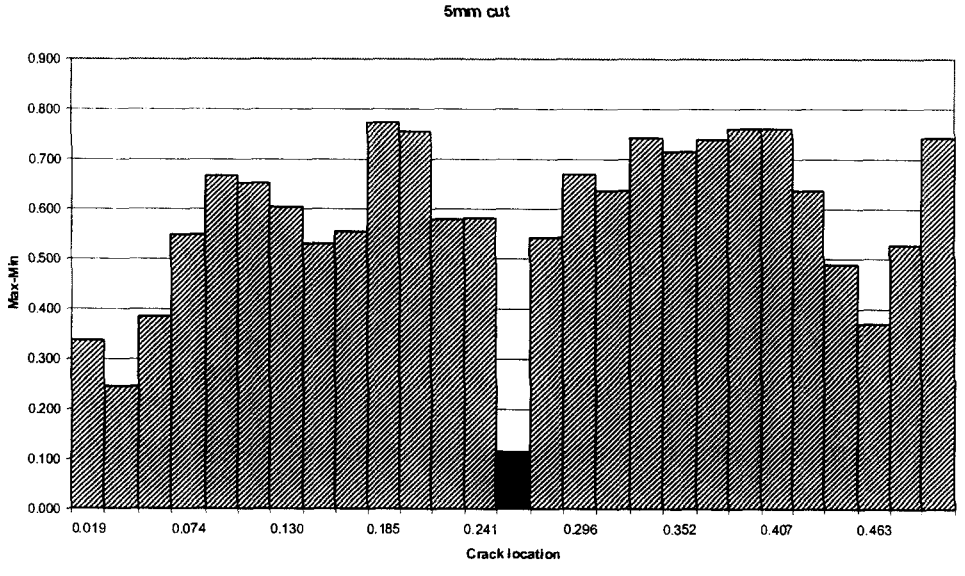

(b)

Figure 5.25 The plots of the difference in normalized *EI* along the beam length, (a) 0.17h cut and (b) 0.28h cut